Wireless Charging of EVs:

Overview and EMC

Jianning Dong, Francesca Grazian and Pavol Bauer

1 November 2022

Agentschap Telecom
Ministerie van Economische Zaken en Klimaat

Amersfoort , The Netherlands

TU Delft

DCE&S
DC systems, Energy conversion & Storage

EV Charging Lab Facilities

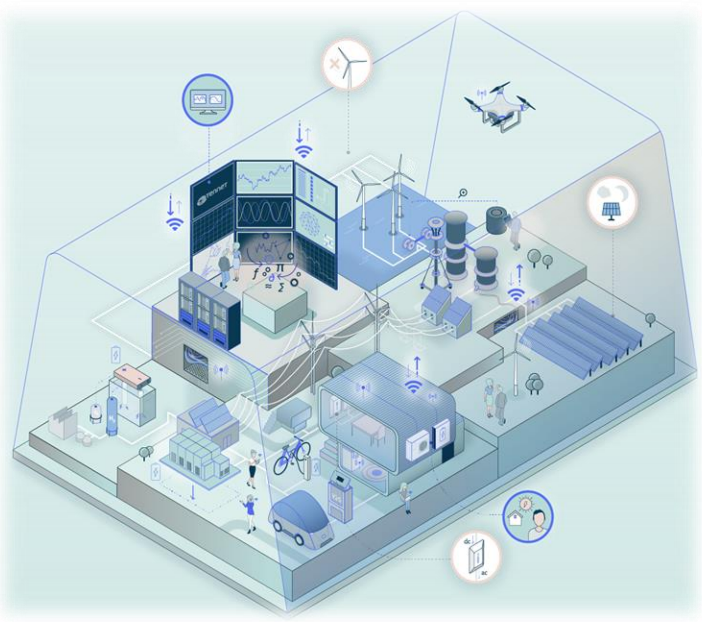

ESP Lab @ TU Delft

Smart Charging
- EV charger emulators

Grid Integration:
- AC&DC grid emulators
- Data loggers triggered by charging events

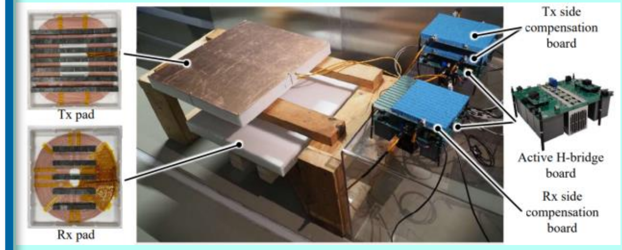

Wireless Charging:
- IPT setup at various power levels
- Dynamic charging platform
- Foreign object detection

Power Modules:
- > 97% efficiency from grid to car
- 2.29 kW/L

TU Delft

DC System, Energy Conversion and Storage (DCE&S) group
Wireless Charging Team

Pavol Bauer
full Professor and DCE&S Head

Jianning Dong
Assistant Professor

Francesca Grazian
Ph.D. candidate

Ph.D. candidates:

Calvin Riekerk

Guangyao Yu

Wenli Shi

Gangwei Zhu

Yi Wang

TU Delft

Outline

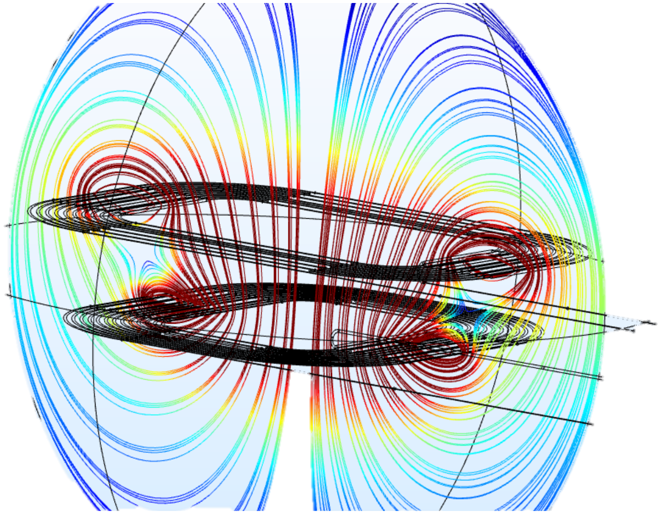

- Introduction and applications
- Inductive power transfer systems
- Design examples
- Standards and Regulations
- EMC and EMF human exposure example
- Conclusion and outlook

TU Delft

Introduction

History

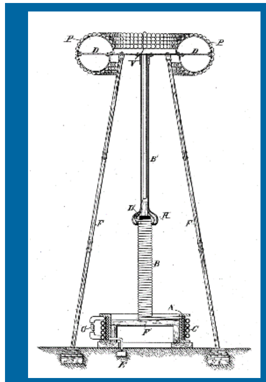

1897:
Tesla WPT patent

1966:
Microwave powered helicopter

Brown, W. C. (1966). The Microwave Powered Helicopter. Journal of Microwave Power, pp. 1–20.

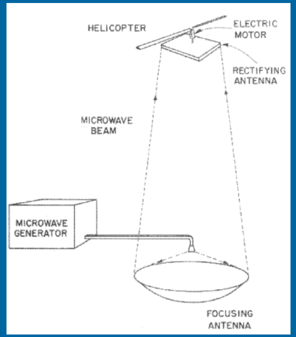

2006:
MIT 2m 60 W WPT experiment

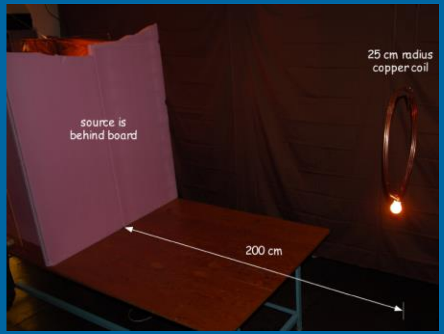

2009:
OLEV by KAIST

1897 – 1917	1950s – 1990s	1990s – early 2000s	2009 – now

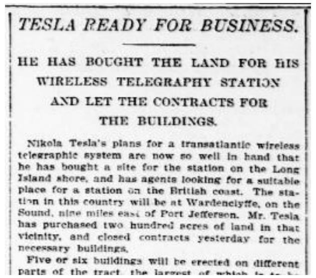

TESLA READY FOR BUSINESS.

HE HAS BOUGHT THE LAND FOR HIS WIRELESS TELEGRAPHY STATION AND LET THE CONTRACTS FOR THE BUILDINGS.

Nikola Tesla's plans for a transatlantic wireless telegraphic system are now so well in hand that he has bought a site for the station on the Long Island shore, and has agents looking for a suitable place for a station on the British coast. The station in this country will be at Wardenclyffe, on the Sound, nine miles east of Port Jefferson. Mr. Tesla has purchased two hundred acres of land in that vicinity, and closed contracts yesterday for the necessary buildings.

Five or six buildings will be erected on different

1901:
Tesla's Wardenclyffe Tower

1970s:
Boom of power electronics

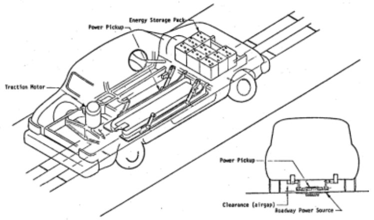

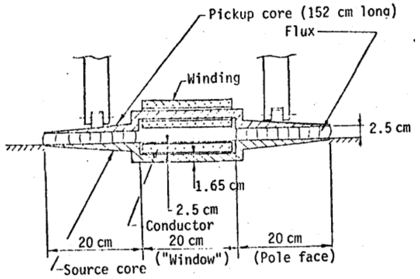

Dynamic charging patents
Otto D. V. (1974), Bolger J. G. (1975)

Fast development of EVs

- Renewed attention for dynamic charging
- Standards defined for wireless charging of EVs
- Commercial development

TU Delft

Classifications of wireless power transfer technologies

Near-Field

- Electric Field
  - Capacitive Coupling
- Magnetic Field
  - Inductive Power Transfer

Far-Field

- Solar
- Micro-Wave
- Lasers
- Radio Wave

Inductive Power Transfer for Electrical Vehicles
www.witricity.com

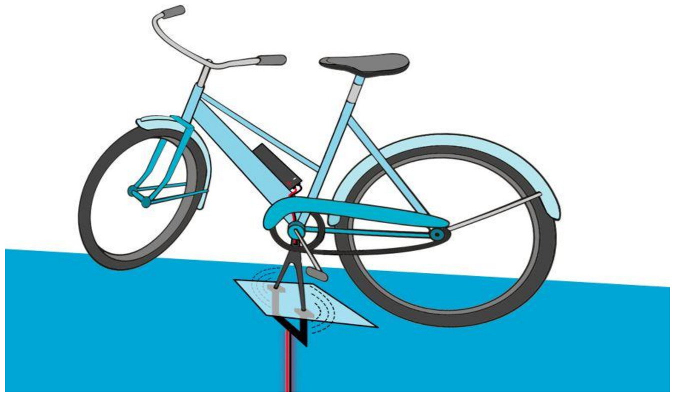

Wireless E-bike Charging
www.tudelft.nl

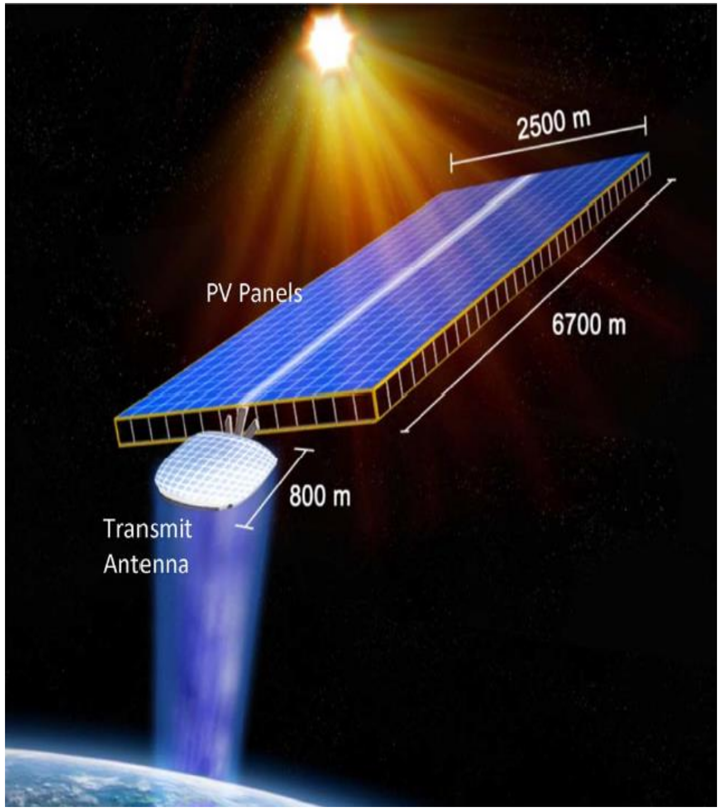

Space Solar Power Transfer

Paul Jaffe et al (2013), “Energy Conversion and Transmission Modules for Space Solar Power”, Proceedings of IEEE, vol. 101, no. 6, 2013

TUDelft

IPT charging: application examples

E-bike charging

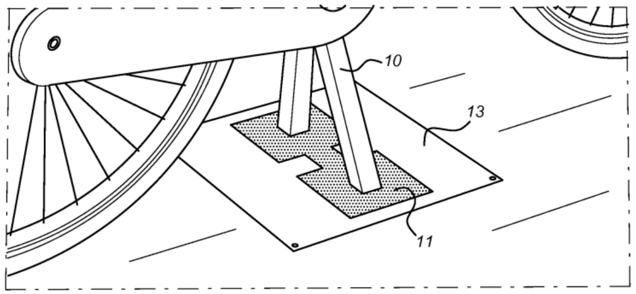

Van Duijsen P., Bauer P. (2017), “Contactless charger system for charging an electric vehicle”, International Patent WO 2018/220164 A1.

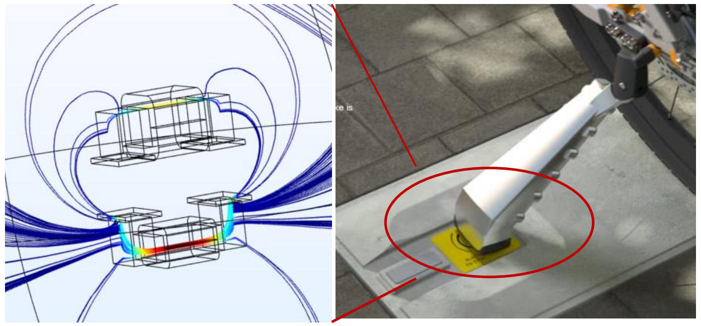

Startup company:
https://www.tilercharge.com/

TU Delft

Bus opportunity charging

200 kW IPT charger

- 1 min charging at stops = 3.3 kWh
- Enough to cover 2.5 km for a rate of 1.3 kWh/km*.

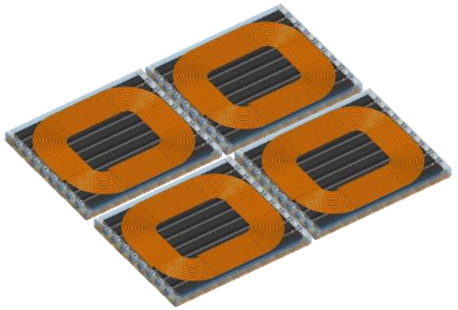

Advantages

- Significant reduction of battery size and weight
- Lower cost and complexity compared to dynamic charging

Research funded by EU project PROGRESSUS
https://progressus-ecsel.eu/

*Based on: Beckers. C. et al (2021), “The State-of-the-Art of Battery Electric City Buses. Paper presented at 34th International Electric Vehicle Symposium and Exhibition (EVS34), Nanjing, China.

Inductive Power Transfer Systems

IPT system topology

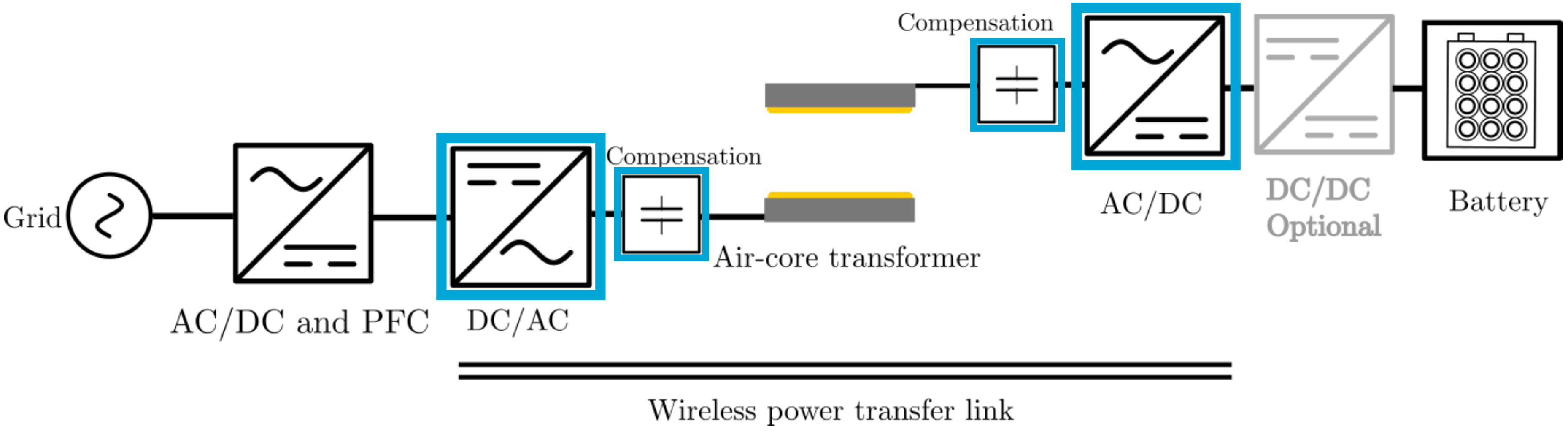

Primary DC/AC

- Current or voltage source
- Half or full bridge

Compensation

- 4 basic ones: series or parallel
  S-S, S-P, P-S, P-P
- High order compensations

Secondary AC/DC

- Current or voltage source
- Half or full bridge
- Active or passive

TU Delft

Induced voltage based transformer model

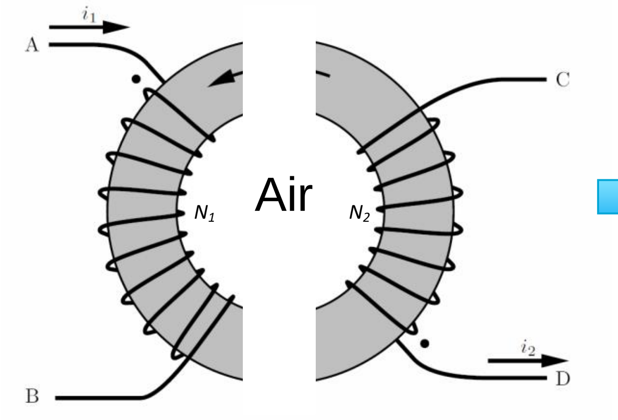

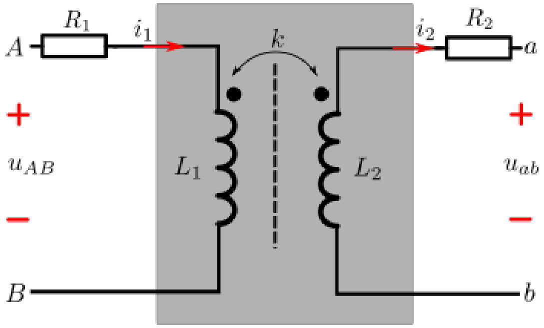

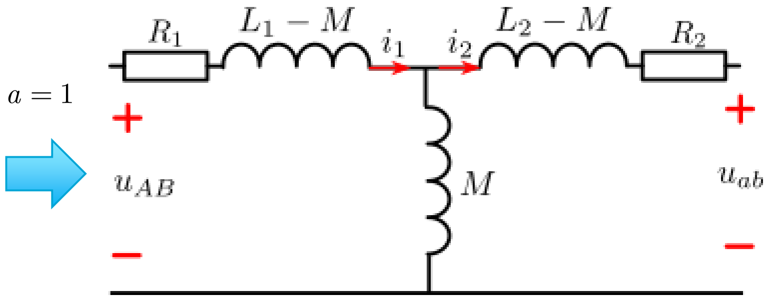

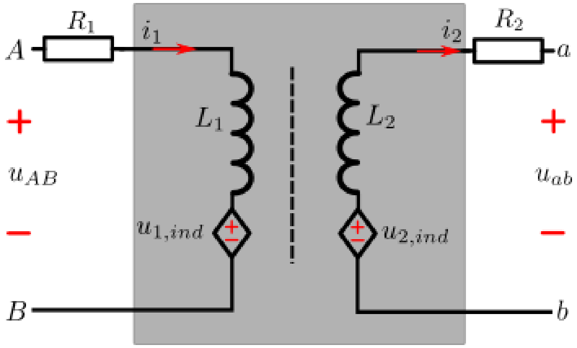

- Large air-gap: lower coupling *k*

$$k = \frac{M}{\sqrt{L_1 L_2}}.$$

$$M = k\sqrt{L_1 L_2}$$

$$u_{1,ind} = -M\frac{\mathrm{d}i_2}{\mathrm{d}t}$$

$$u_{2,ind} = M\frac{\mathrm{d}i_1}{\mathrm{d}t}$$

Transferred power through air gap at steady state

$$P_{12} = \Re\{j\omega M \underline{I}_1 \underline{I}_2^*\} = \omega M I_1 I_2 \sin\phi_{12}$$

Valid for all compensations

$\underline{I}_1,\ \underline{I}_2$ – primary/secondary current phasors

ϕ_{12} – $\underline{I}_1,\ \underline{I}_2$ phase difference

TUDelft

Compensations

- 4 basic ones: series or parallel

  S-S, S-P, P-S, P-P

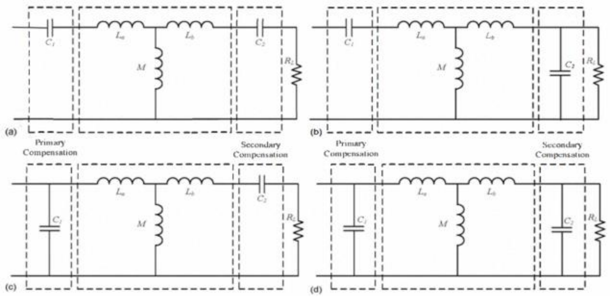

Chopra S., Bauer P. (2011), "Analysis and design consideration for a contactless power transfer system", 33rd INTELEC.

- Voltage source converters for S
- Current source converters for P

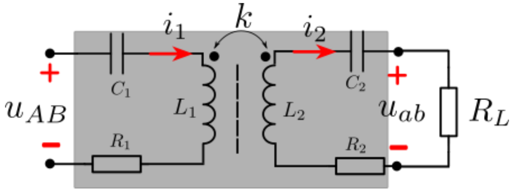

AC link of S-S compensation

$$C_1 = \frac{1}{\omega^2 L_1}, \quad C_2 = \frac{1}{\omega^2 L_2}$$

$$I_2 \approx \frac{U_{AB}}{\omega M}, \quad \frac{U_{ab}}{U_{AB}} \approx \frac{R_L}{\omega M}$$

- High order compensations
  - SP-S, LCC-S, double LCC …
  - More flexibility
  - More components to share voltage stress?
  - Configured to realize different voltage/current source behaviours

Wang Z., Mi C. (2016), "Compensation topologies of high-power wireless power transfer systems", IEEE TVT, vol. 65, no.6.

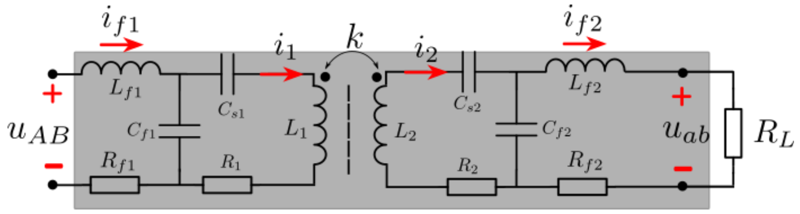

AC link of double side LCC (DLCC) compensation

$$C_{si} = \frac{1}{\omega^2 (L_i - L_{fi})}, C_{fi} = \frac{1}{\omega^2 L_{fi}}, \quad i = 1, 2$$

$$I_{f2} \approx \frac{M U_{AB}}{\omega L_{f1} L_{f2}}, \quad \frac{U_{ab}}{U_{AB}} \approx \frac{M R_L}{\omega L_{f1} L_{f2}}$$

TU Delft

Converters

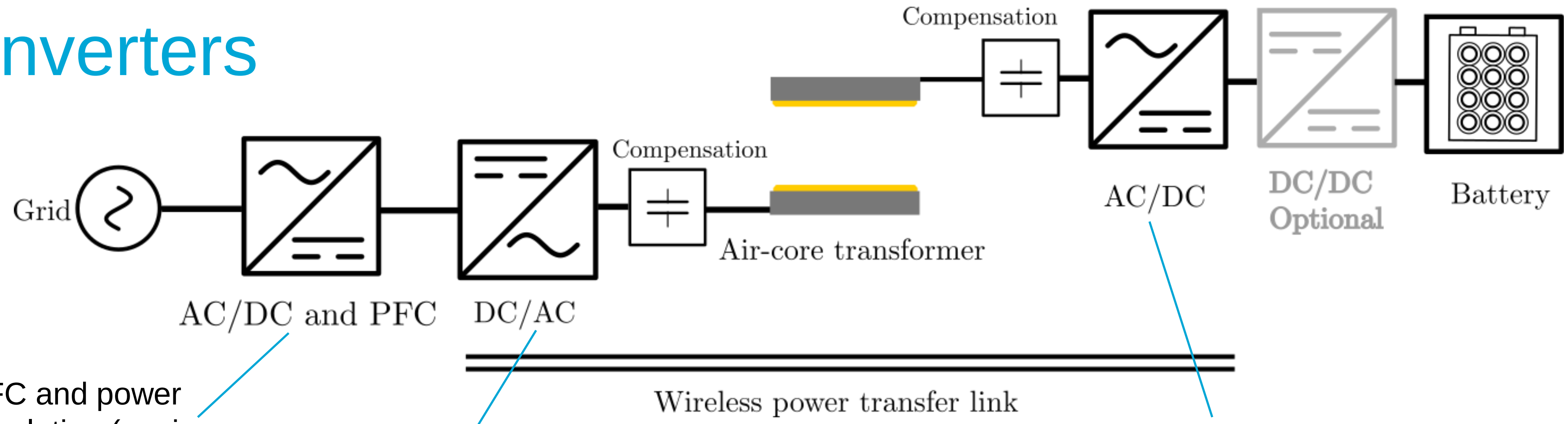

PFC and power regulation (or via a front-end DC-DC)

- Passive rectifier
- Semi-active/active rectifier
- VS/CS depending on compensation

Voltage/current source inverters depending on compensation

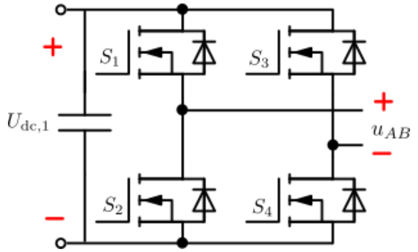

- No phase shift: wide range soft-switching, DC voltage regulated
- Phase shift control for power regulation (soft switching?)

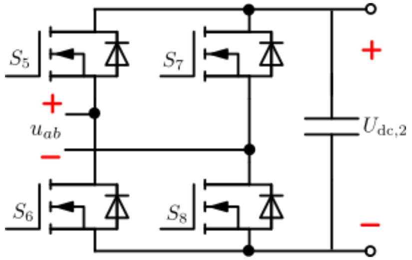

- Synchronous rectification
- Phase shift control for load matching (soft switching?)

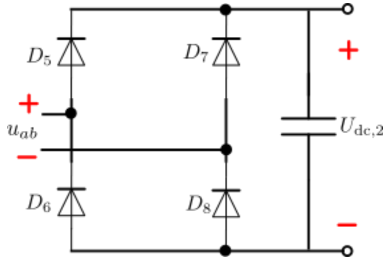

- Fixed impedance transformation ratio

TU Delft

Loss distribution

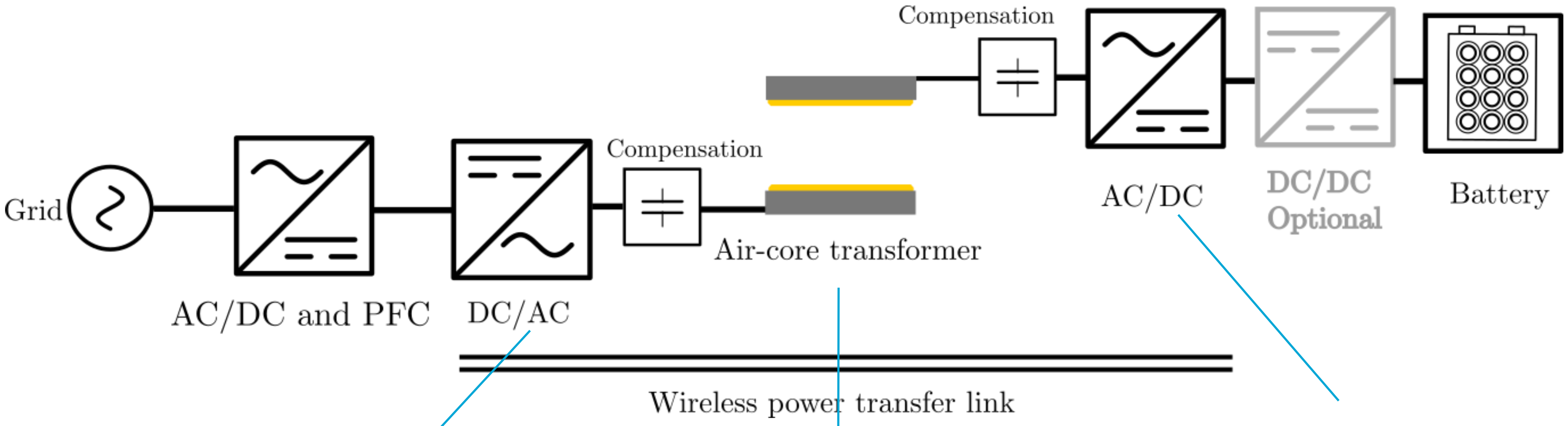

P_{inv}:

Loss in power semiconductors

P_{c}:

P_{com}: compensation loss, parasitic resistances
P_{coil} : coil copper loss, DC+skin effect+approximity loss
P_{fe} : core loss, hysteresis
P_{sh} : shielding loss, eddy current loss

P_{rec}:

Loss in power semiconductors

Multi-objective optimization

Search space

- Dimensions
- Number of turns/strands/coil diameter
- Core material/shielding material
- Compensation topology
- Core arrangement
- …

IPT system model

- 3D FEA, inductance evaluation
- Circuit model
- Loss models
- Weight/volume calculation
- …

Conflicting objectives

- Aligned efficiency
- Stray field
- Gravimetric power density
- Area power density
- …

Multi-objective optimizer

- Genetic algorithm
- Particle swarm
- …

Pareto fronts

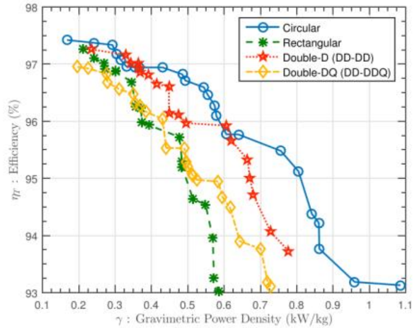

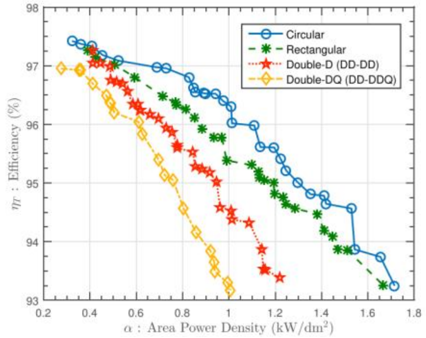

Bandyopadhyay S., et al. (2019), "Comparison of Magnetic Couplers for IPT-Based EV Charging Using Multi-Objective Optimization," *IEEE TVT*, vol. 68, no. 6, pp. 5416–5429.

TU Delft

Design Examples

High efficiency 3.7 kW IPT system

Variable series compensation capacitor

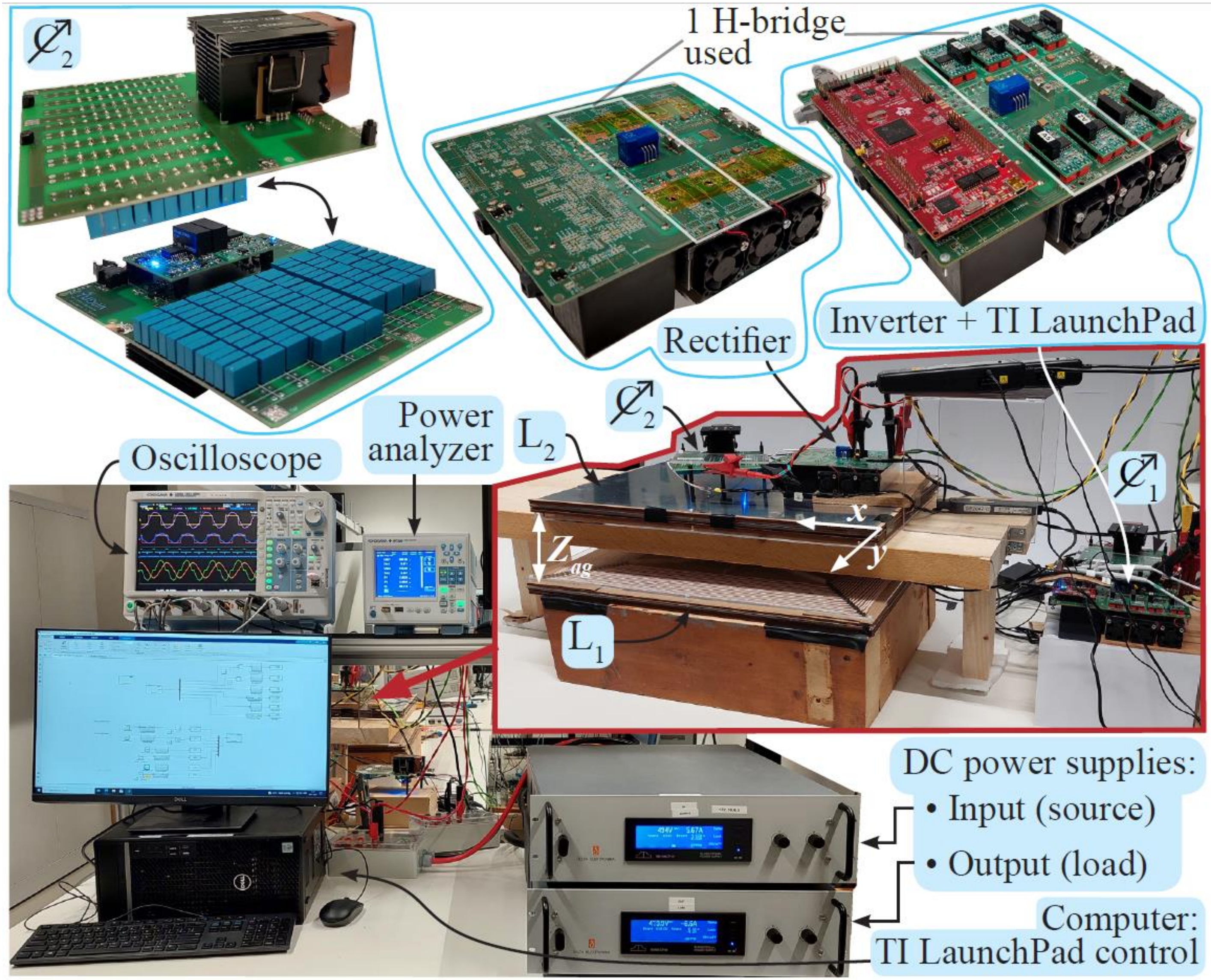

Switch-controlled capacitor (SCC) as compensation

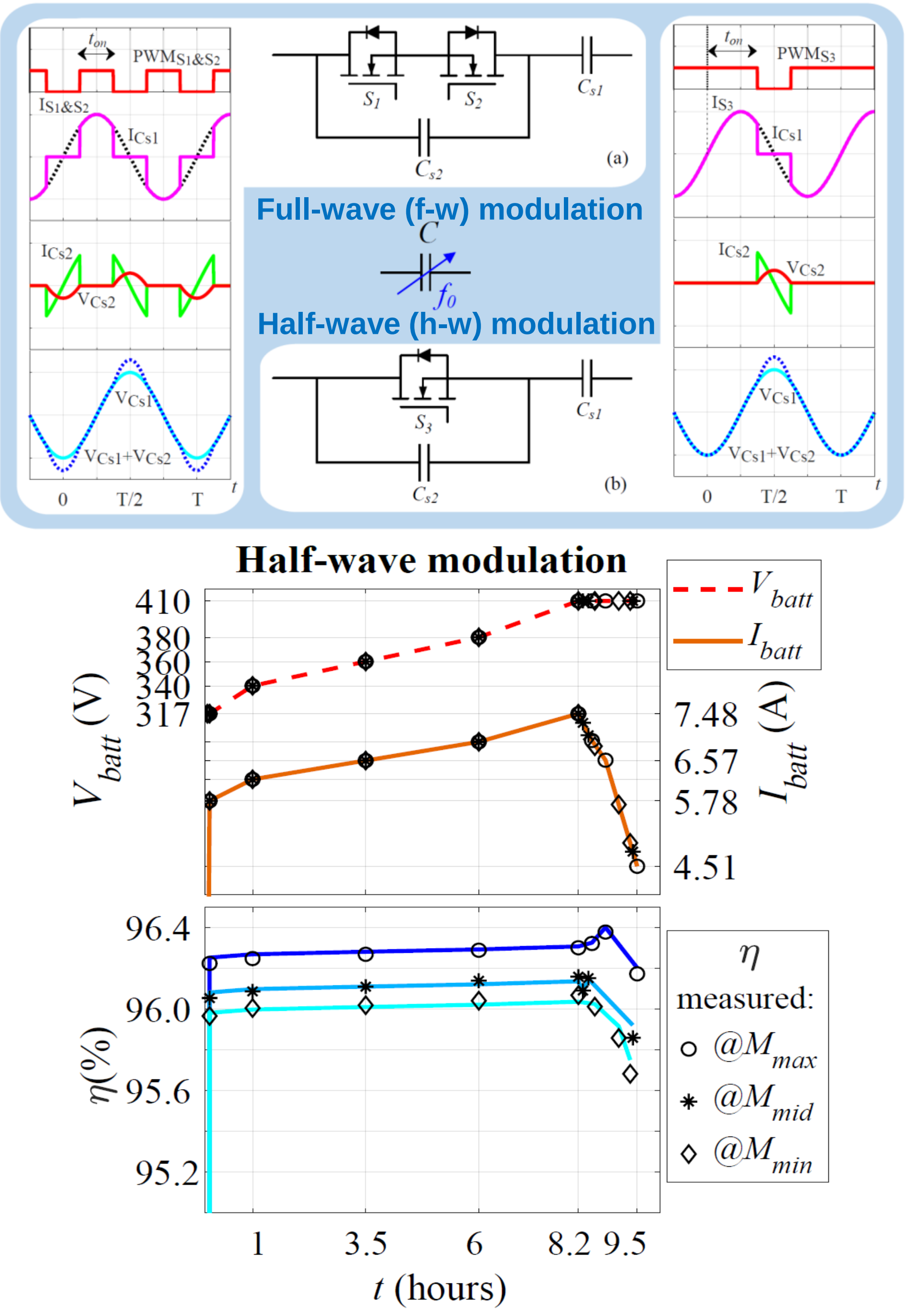

7.7 kW IPT system universal for 400V and 80V batteries

Voltage/current doubler (V/I-D) converter → *Multicoil design*

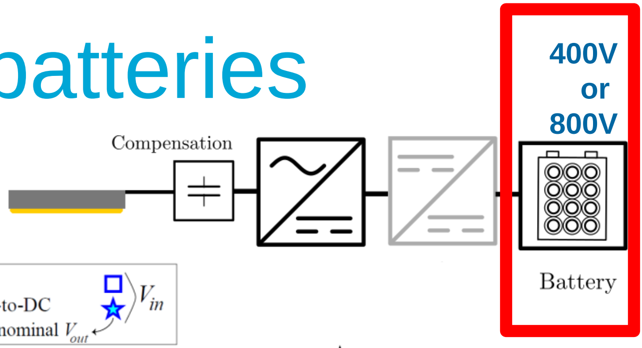

2 sets of rectangular coils

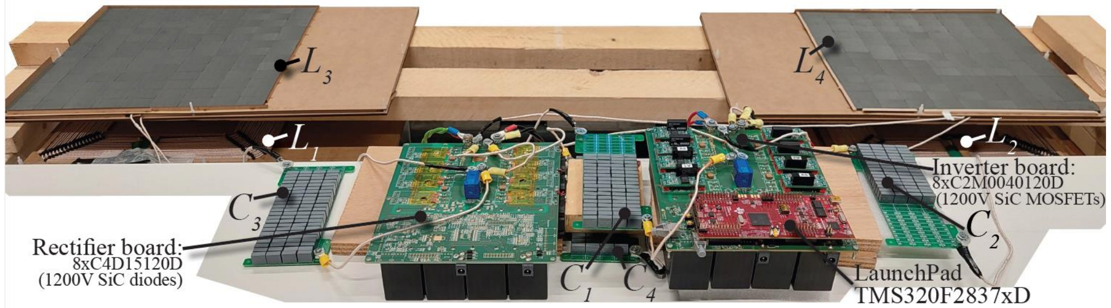

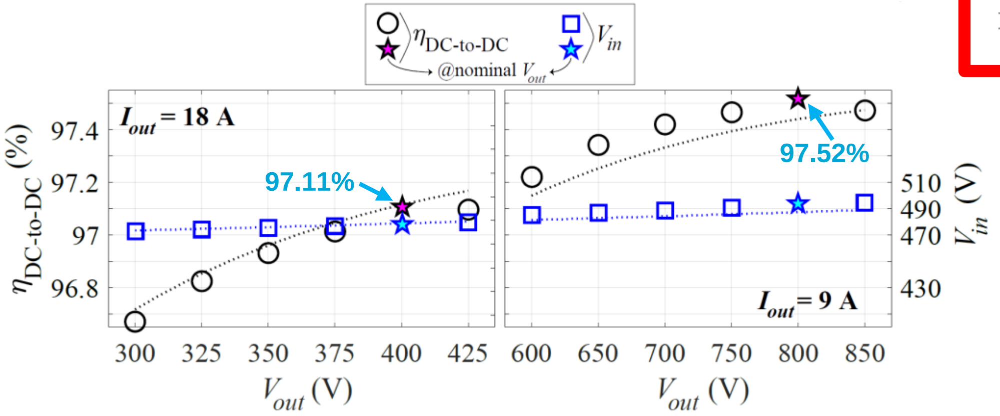

Bipolar pads (BPPs) → Compact solution

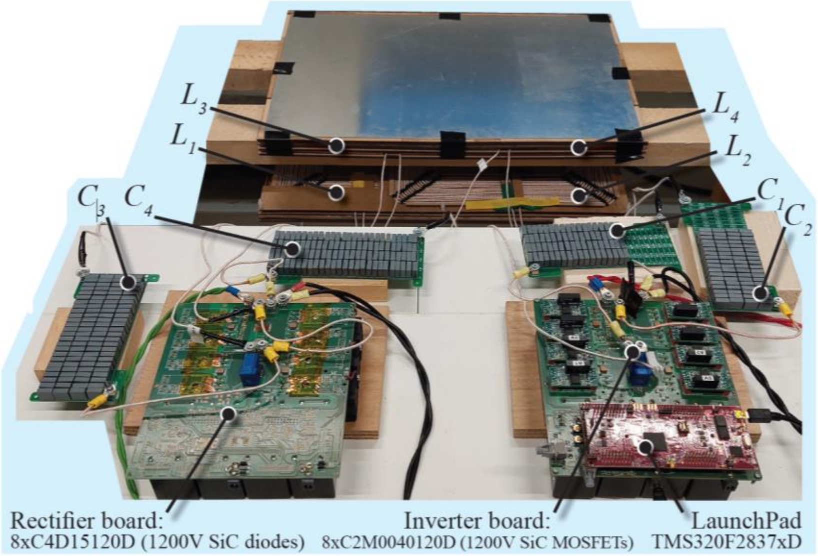

Slight efficiency difference between the two charging modes!

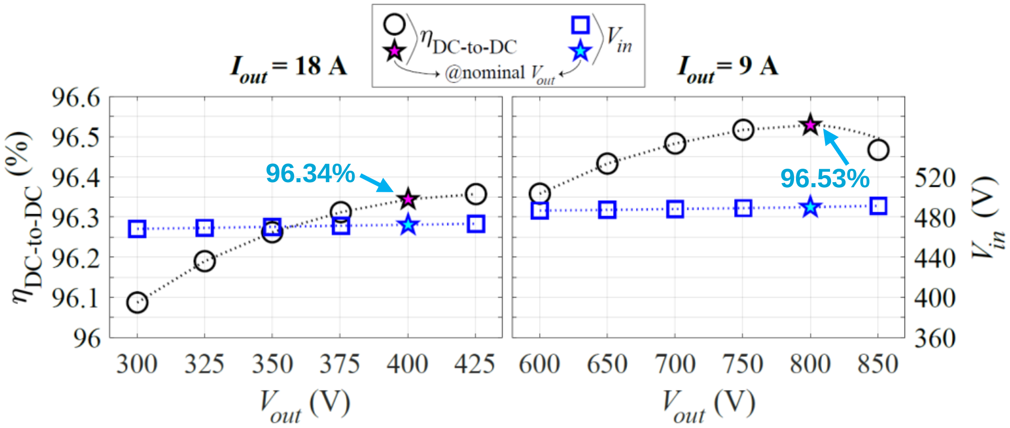

TU Delft

High efficiency 20 kW IPT system

Test result

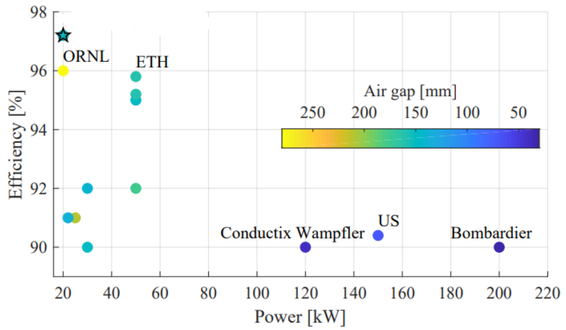

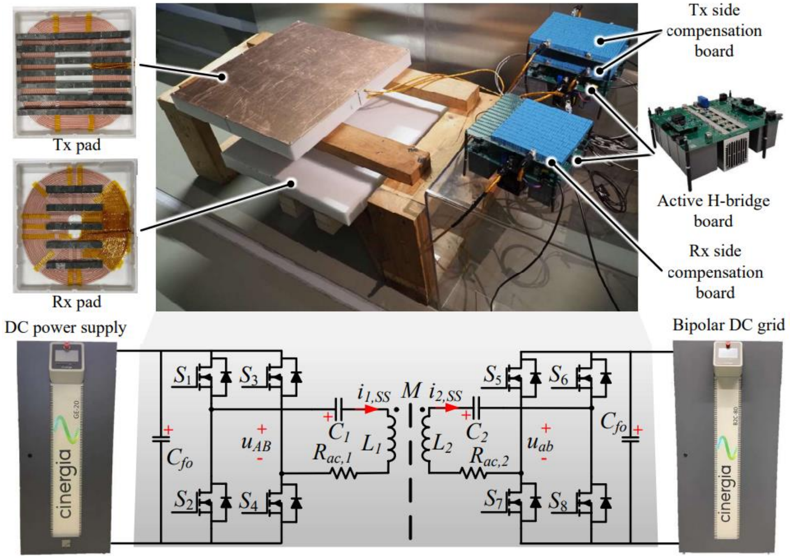

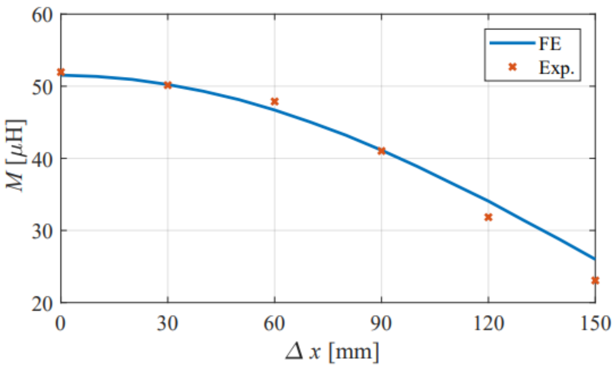

Inductance measurement vs. FEA

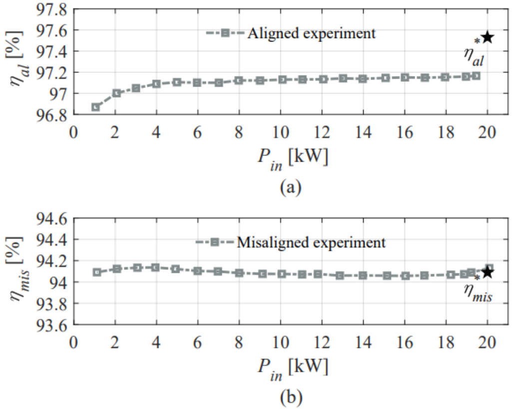

Efficiency measurement vs. analysis

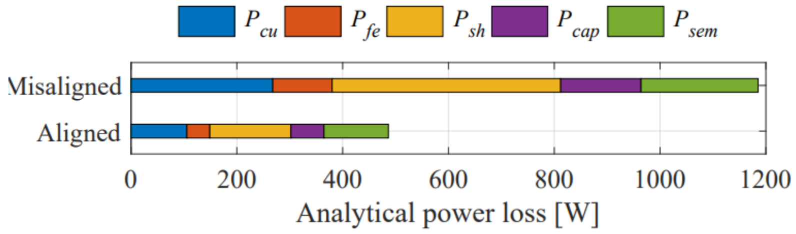

Loss breakdown

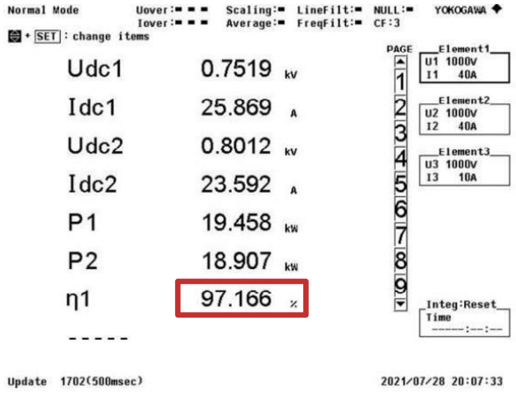

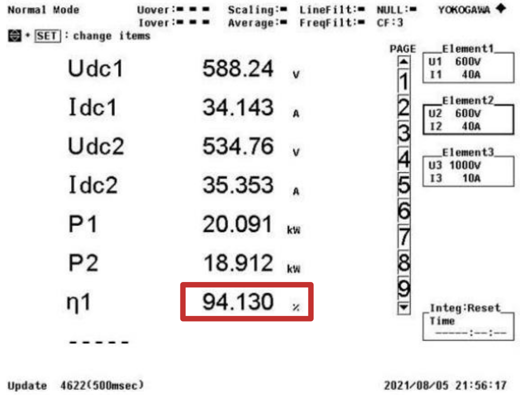

Aligned and misaligned efficiency

TU Delft

Standards and Regulations

Available Standards and Regulations

From 2015 until now:

- IEC 61980 series
- ISO 19363
- SAE J2954
- SAE J2847/6
- IEC PAS 63184

TUDelft

Available Standards and Regulations

From 2015 until now:

- IEC 61980 series
- ISO 19363
- SAE J2954
- SAE J2847/6
- IEC PAS 63184

Electric vehicle WPT systems

- IEC 61980-1 - Part 1: **General** requirements
  1st Edition 2015 – 2nd Edition 2020

- IEC TS 61980-2 - Part 2: Specific requirements for **communication** between electric road vehicle (EV) and infrastructure
  TS in 2019 – forecast 1st Edition 2023

- IEC TS 61980-3 - Part 3: Specific requirements for **magnetic field** wireless power transfer (MF-WPT) systems
  TS in 2019 – forecast 1st Edition Dec 2022

IEC 61980-1

Defines the generic aspects of WPT common to:

- Inductive power transfer (also magnetic resonance);
- Capacitive Power Transfer;
- Microwave Power Transfer (1-300 GHz);
- Infrared Power Transfer (300 GHz-400 THz).

→ **EMC limits for disturbances**

Categorization of EMC disturbances according to IEC 61980-1.

Port	**Phenomenon**	**Frequency range**
AC power input	Conducted disturbances	150 kHz to 30 MHz
Wired network		150 kHz to 30 MHz
Enclosure	Radiated disturbances	9 kHz to 150 kHz
		150 kHz to 30 MHz
		30 MHz to 1 GHz

Available Standards and Regulations

From 2015 until now:

- IEC 61980-2
- ISO 19363
- SAE J2954
- SAE J2847/6
- IEC PAS 63184

➢ **Communication** between Wireless Charged Vehicles and Wireless EV Chargers
RP in 2015 – 1st Edition 2020

Available Standards and Regulatio

From 2015 until now:

- IEC 61980 series
- ISO 19363
- SAE J2954
- SAE J2847/6
- IEC PAS 63184

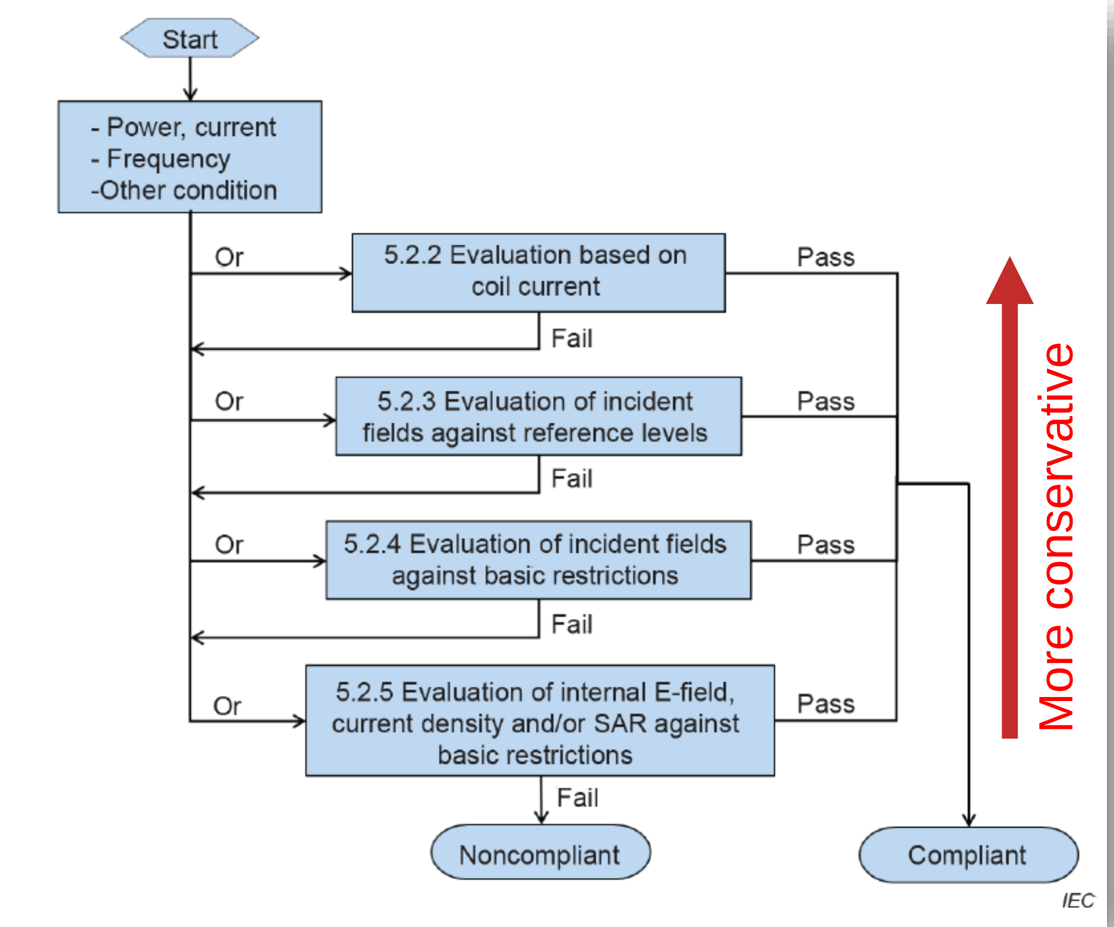

- **Assessment methods of the human exposure** to electric and magnetic fields from wireless power transfer systems – Models, instrumentation, measurement and numerical methods and procedures (frequency range of 1 kHz to 30 MHz)
  PAS (pre-standard) in 2021

TU Delft

Available Standards and Regulations

- IEC 61980-3
- ISO 19363
- SAE J2954
- SAE J2847/6
- IEC PAS 63184

→ WPT with magnetic resonance

→ Stationary

→ Unidirectional

→ Surface-mounted

Available Standards and Regulations

- IEC 61980-3
- ISO 19363
- SAE J2954
- SAE J2847/6
- IEC PAS 63184

- Electrically propelled road vehicles - Magnetic field wireless power transfer - Safety and interoperability requirements
  PAS in 2017 – 1st Edition in 2020
- Wireless Power Transfer for Light-Duty Plug-In/ Electric Vehicles and Alignment Methodology
  TIR in 2016 – RP in 2017 – 1st Edition 2020 – 1st Edition revised in 2022

IEC 61980-3, ISO 19363, SAE J2954

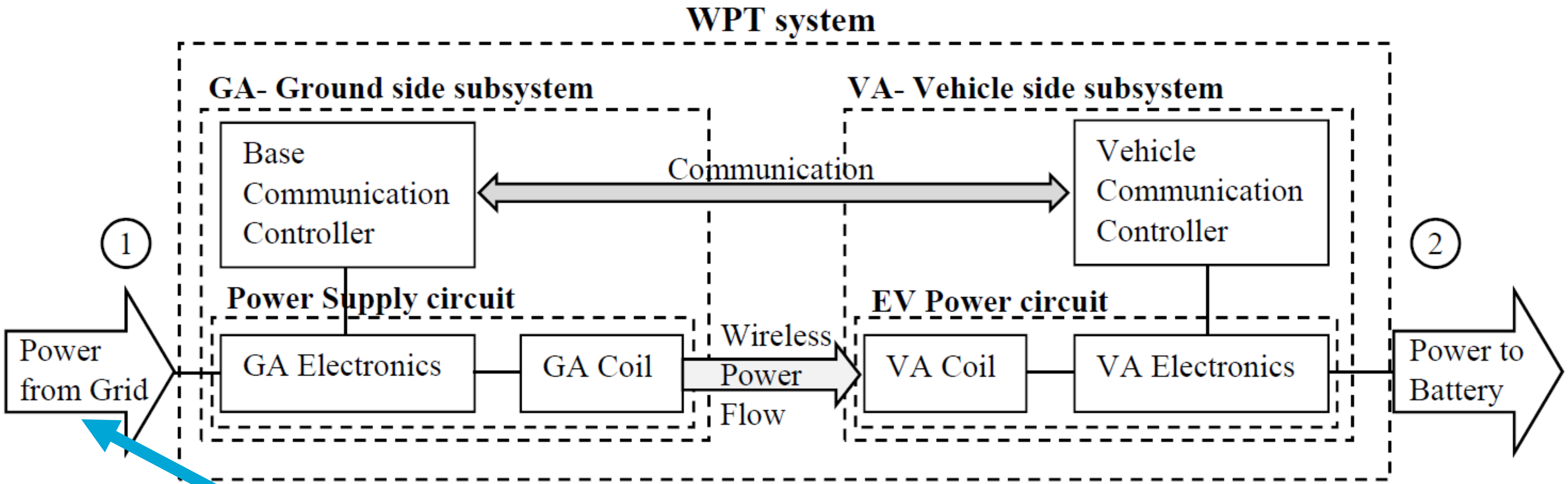

	Power classes				
	WPT1	WPT2	WPT3	WPT4*	WPT5*
Maximum input (kVA)	3.7	7.7	11.1	22	60
*under consideration					

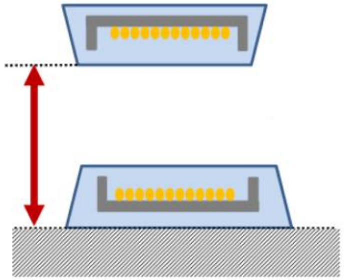

		Z-classes		
		Z1	Z2	Z3
VA Coil ground clearance range (mm)	from	100	140	170
	to	150	210	250

Minimum efficiency betwee ① and ② :

→ 85 % aligned

→ 80 % offset

IEC 61980-3, ISO 19363, SAE J2954

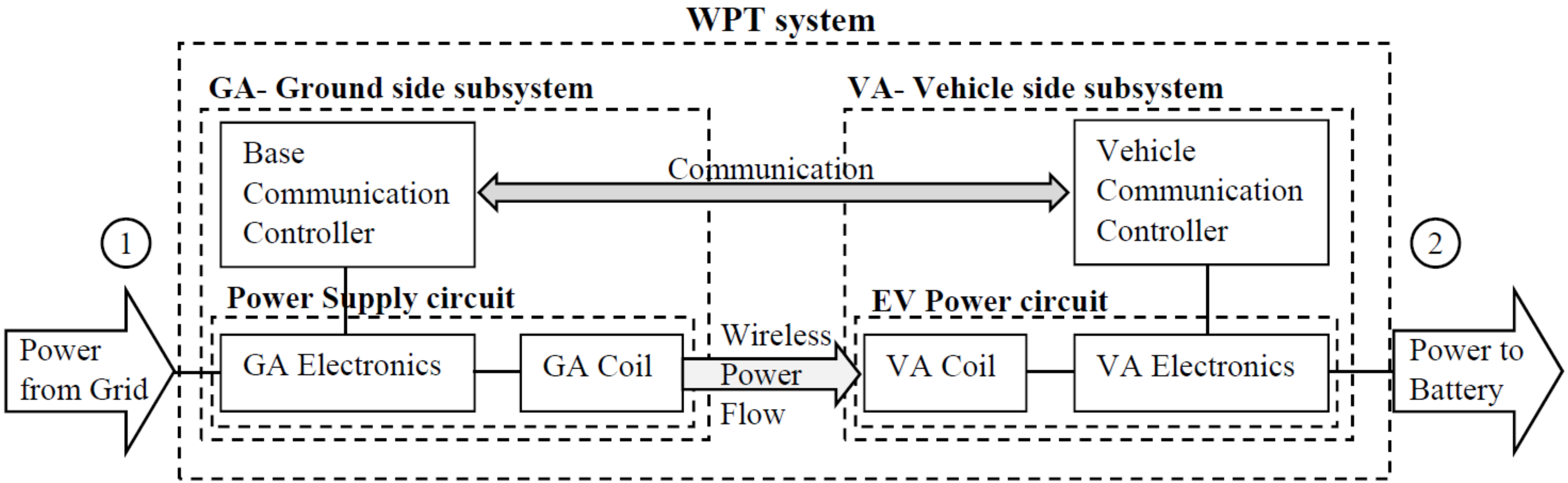

- Operating frequency

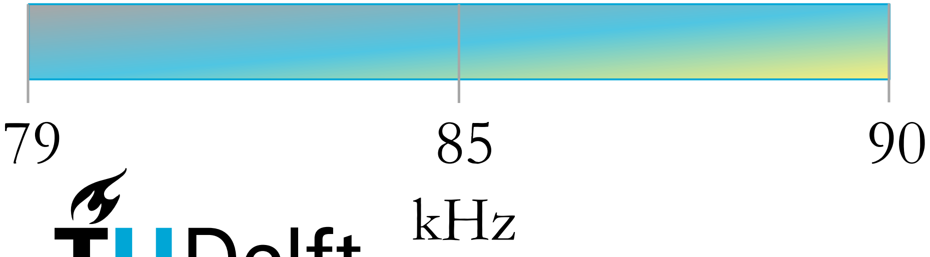

- Offset tolerances

Direction	Value
ΔX	±75 mm
ΔY	±100 mm
ΔZ	Zmax, Zmin ∈ Z-class
Roll, Pitch, Yaw	±2°, ±2°, ±3°

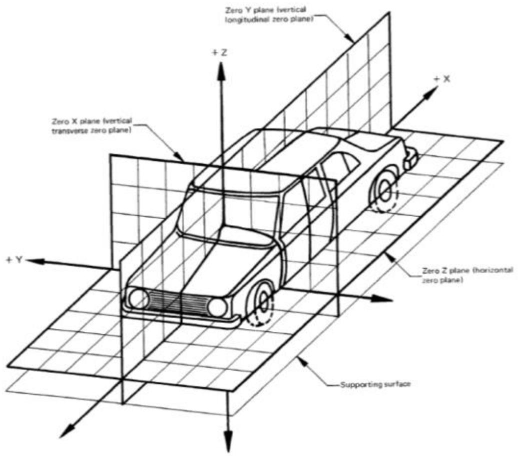

TU Delft

IEC 61980-3, ISO 19363, SAE J2954

- Electromagnetic Compatibility (EMC)

→ Immunity → Conducted
→ **Disturbance** → **Radiated**

- EMF human exposure

→ at the worst misalignment and maximum power

- **ICNIRP Guideline 2010 for General Public**

Electric field strength - E	Magnetic field strength - H	Magnetic flux density - B	Contact current
83 V/m	21.5 A/m	27 μT	$0.2 * f$(kHz) =17 mA @85 kHz

(RMS values)

- **AAMI/ISO 14117-2012 Annex M for pacemakers**

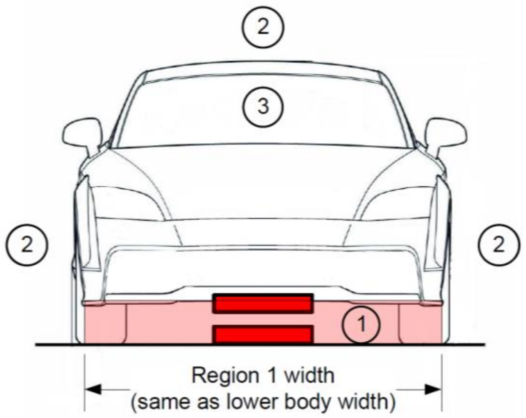

Magnetic filed strength - H	Magnetic flux density - B
11.9 A/m	15 μT
from 79 to 90 kHz	

(RMS values)

TU Delft

IEC 61980-3, ISO 19363, SAE J2954

EMC (radiated disturbance)

- IEC 61980-1
- ISO 19363

→ CISPR 11 Group 2*

<u>Environmental</u>

↗ Class A (non-residential)

↘ Class B (residential)

- SAE J2954 → proposed Recommended Limits

*A specific part of CISPR 11 for WPT is under development

IEC 61980-3, ISO 19363

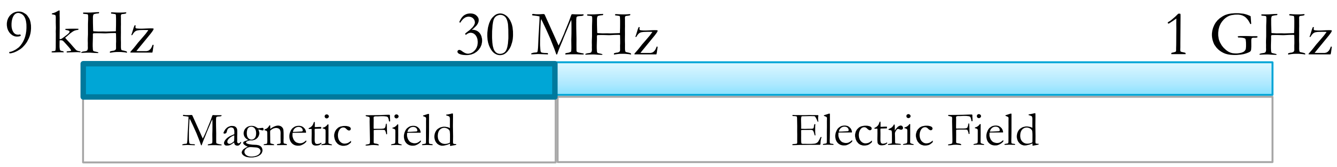

EMC (radiated disturbance)

9 kHz-150 kHz

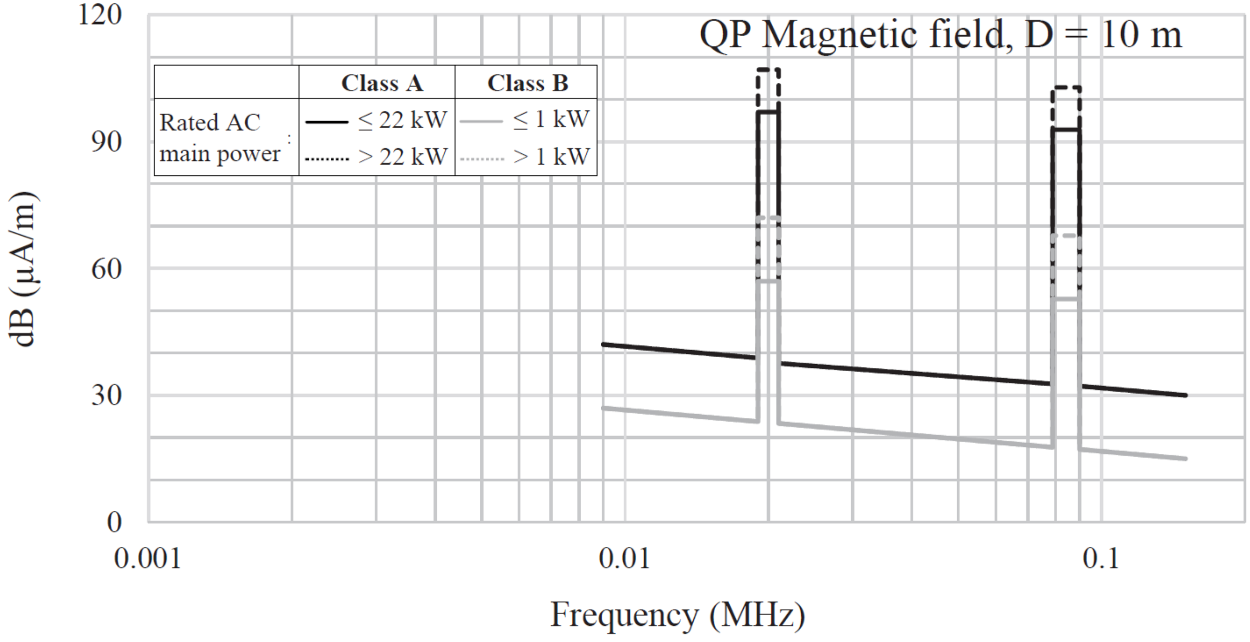

150 kHz-30 MHz

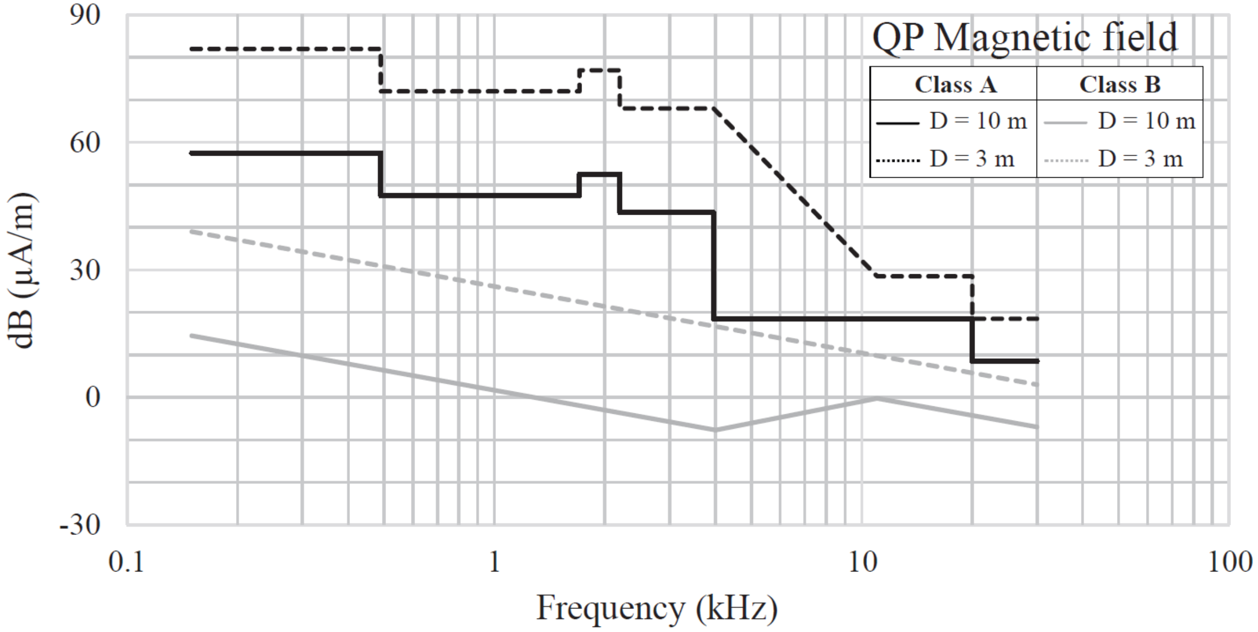

IEC 61980-3, ISO 19363

EMC (radiated disturbance)

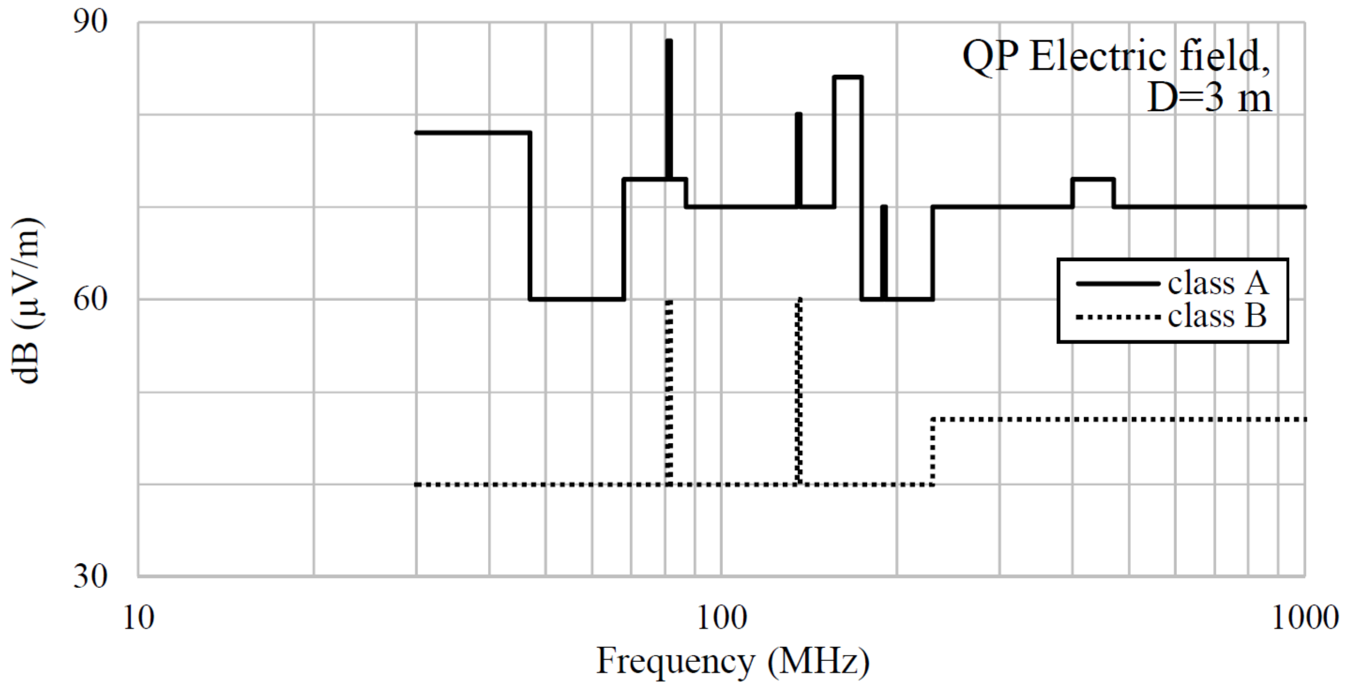

TU Delft

SAE J2954

EMC (radiated disturbance)

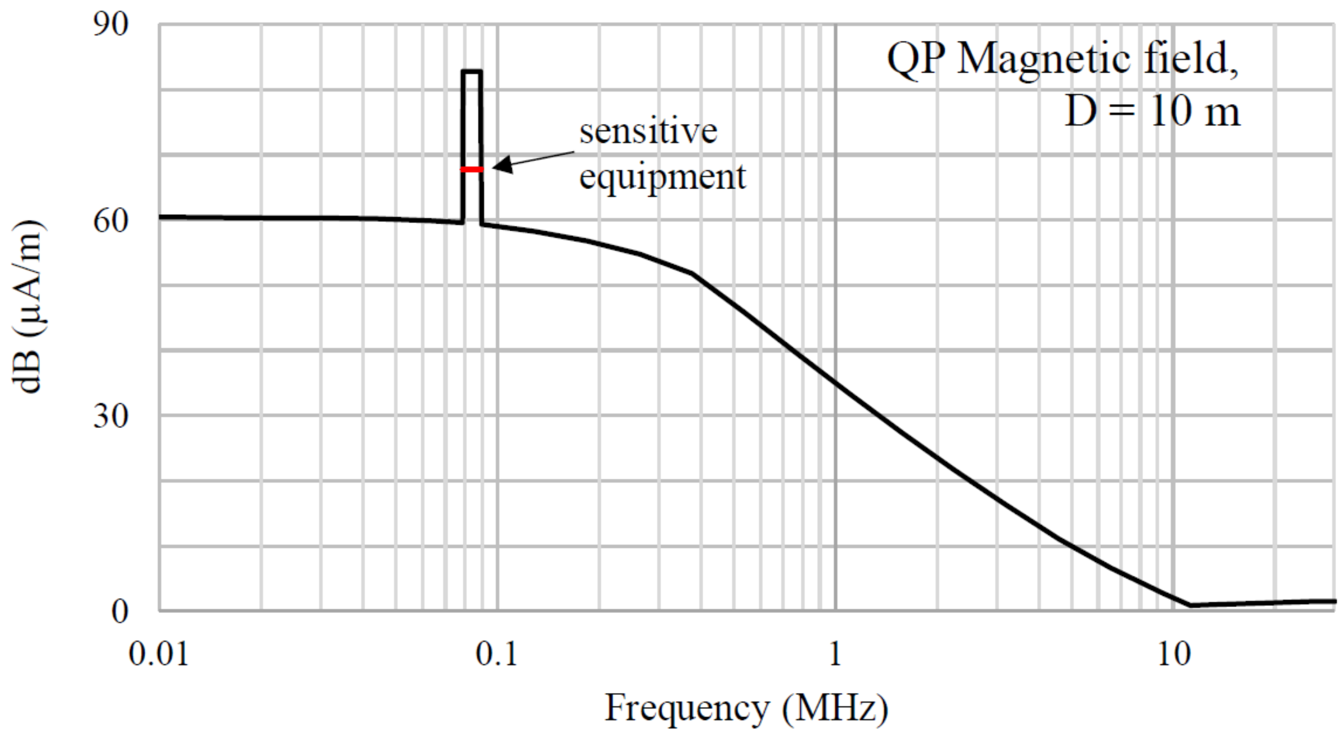

IEC 61980-3, ISO 19363, SAE J2954

EMC (radiated disturbance) - Comparison

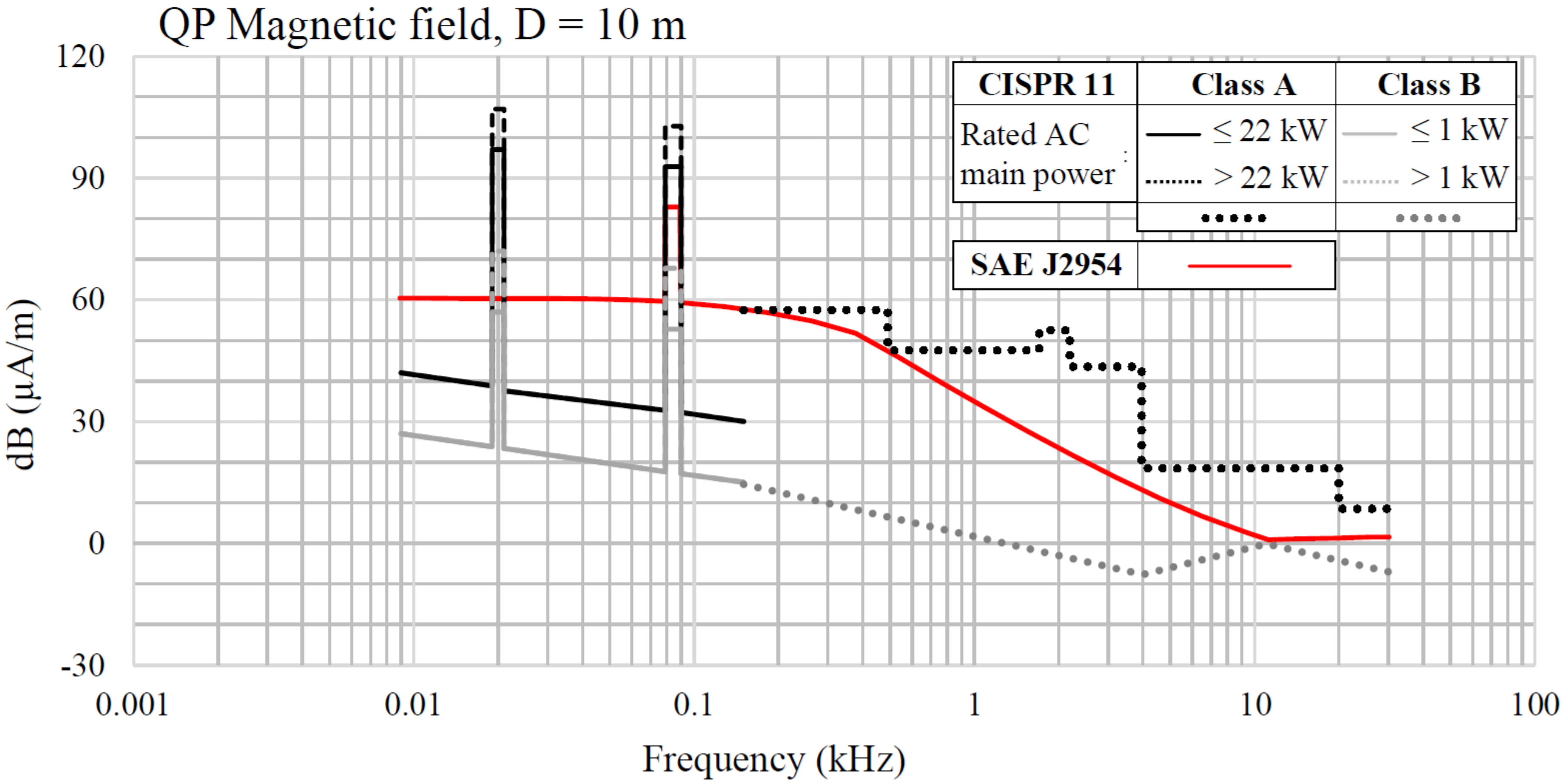

TU Delft

EMC and EMF human exposure example

Constant optimum load through variable series compensation

3.7kW lab prototype

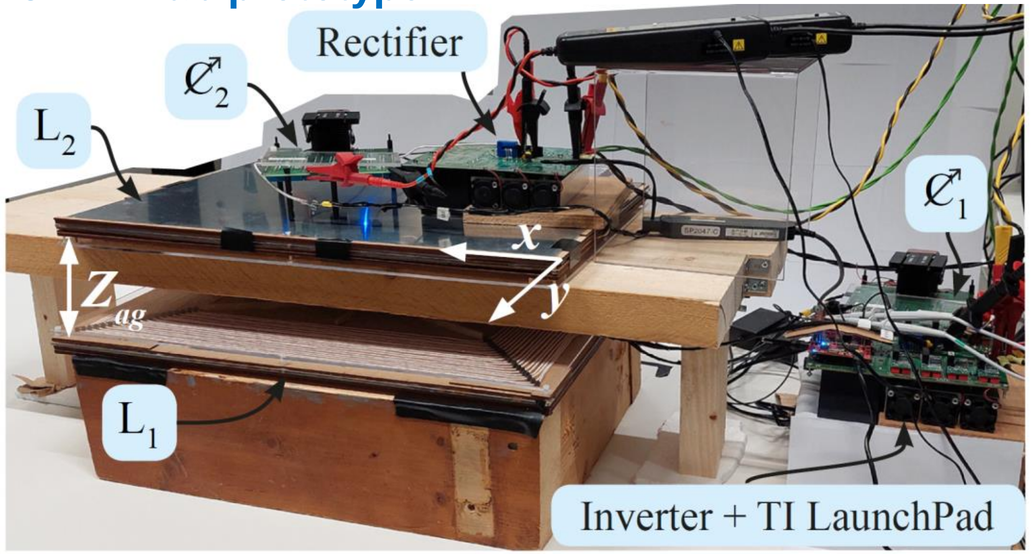

V_{out} (V)	317...410	Devices: M1...M4	C2M0040120D
I_{out}: CC, COL (A)	7, 7.48	D1...D4	C4D15120D
V_{in} (V)	360...515	S1...S3	C2M0045170P
f_0 (kHz)	79...90	C unit	B32671L
L_1, L_2 (μH)	336.9, 224.2	M_{min}, M_{mid}	90.1, 95.4
C_{s1_1}, C_{s1_2} (nF)	13.50, 18.57	M_{max} (μH)	102.6
C_{s2_1}, C_{s2_2} (nF)	28.03, 52.08	C_1, C_2 (nF)	15.14, 18.55

I_1, I_2: Symmetrical distortion

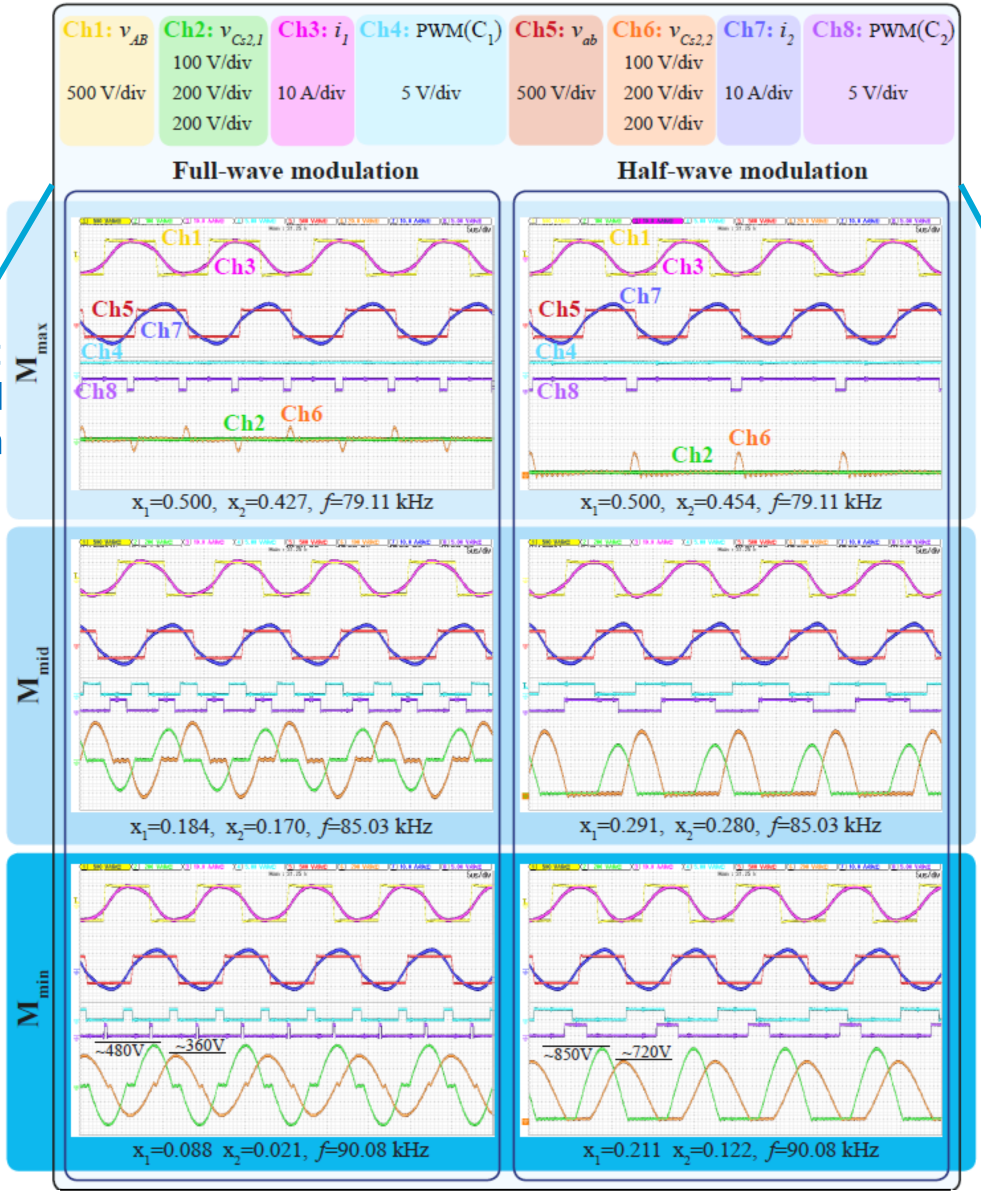

I_1, I_2: Asymmetrical distortion

Measured circuit waveform

TU Delft

Measured current distortion

	THD(I_1) (%)			THD(I_2) (%)		
	M_{min}	M_{mid}	M_{max}	M_{min}	M_{mid}	M_{max}
SCC: f-w	6.84	7.83	7.28	7.11	8.38	8.14
SCC: h-w	7.89	10.57	7.37	7.36	10.98	8.16
const C	6.16	6.65	7.69	8.16	8.51	9.04

→ Considered in the next analysis

SCC with h-w modulation: highest THD

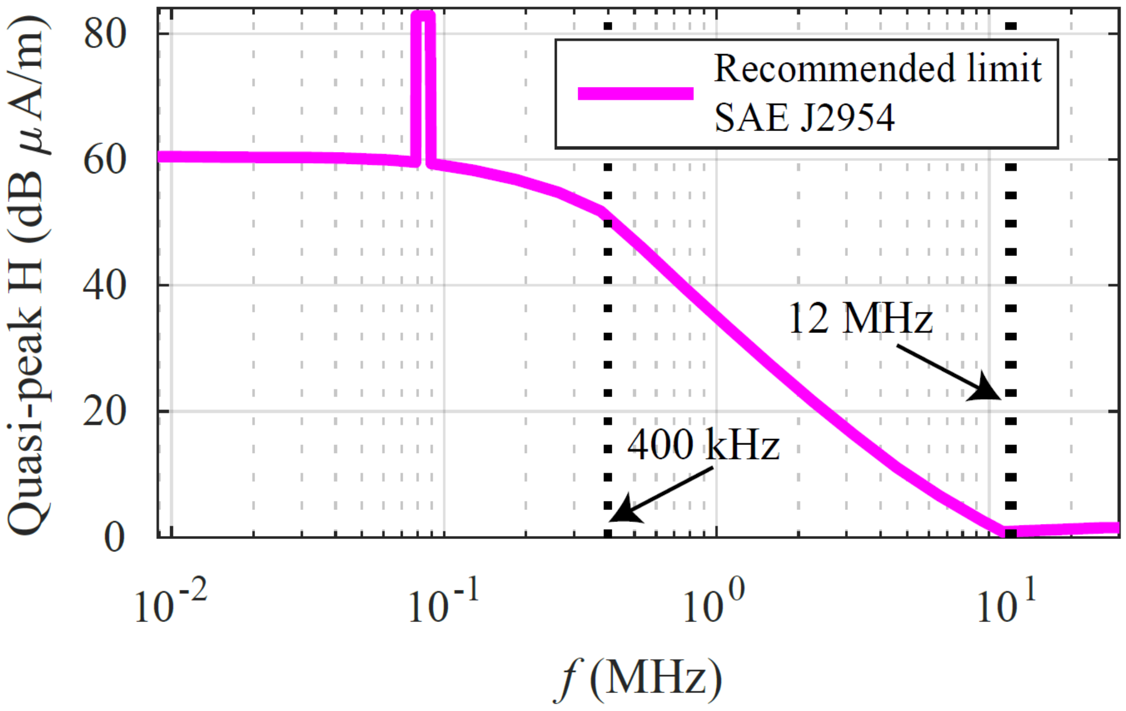

TU Delft

Measured current distortion

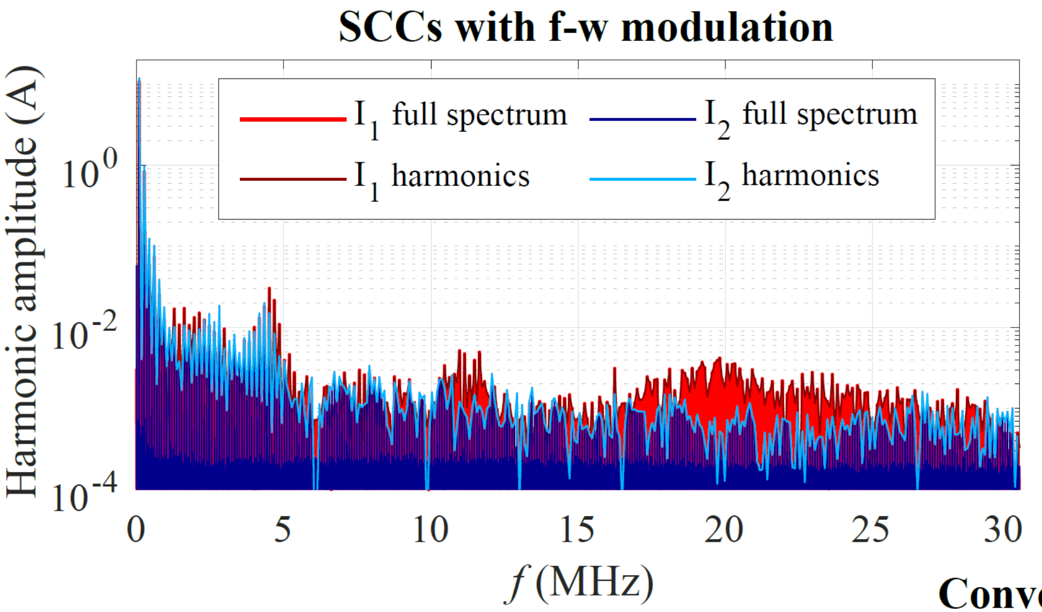

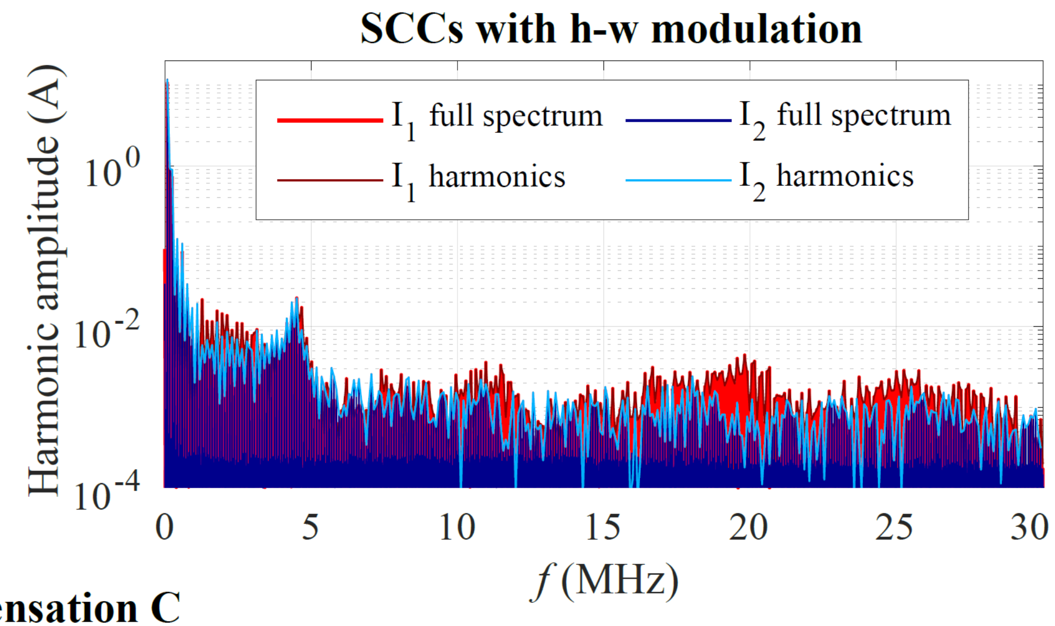

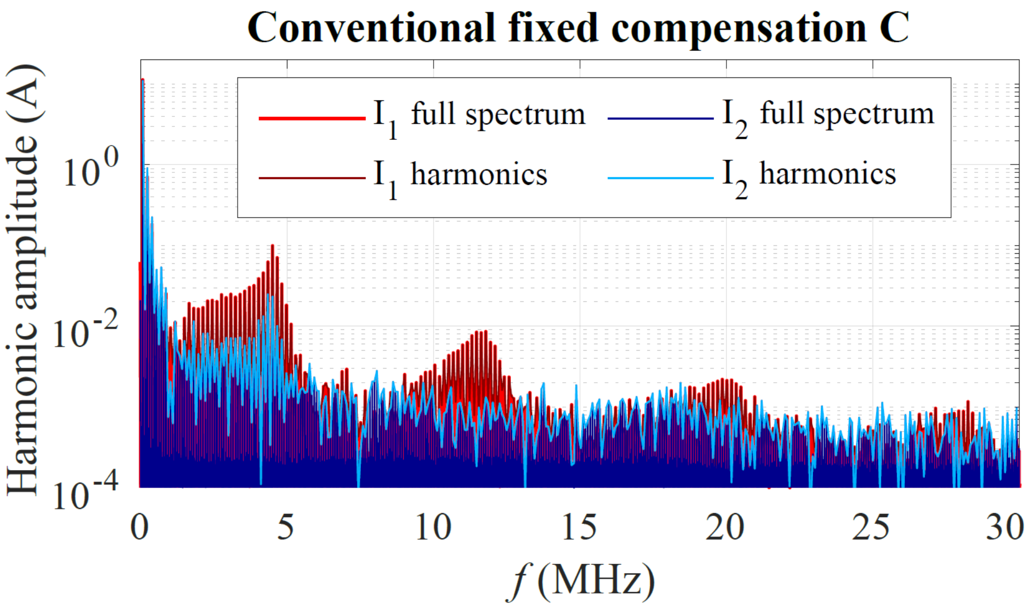

I_1 shows more critical harmonic amplitudes than I_2

TU Delft

Measured current distortion

SCC with h-f modulation has higher THD.

However, the harmonic amplitudes at the critical frequencies of the SAE J2954 recommended limit are comparable to the other implementations.

FFT of I_1: SCC with f-w and h-w modulation

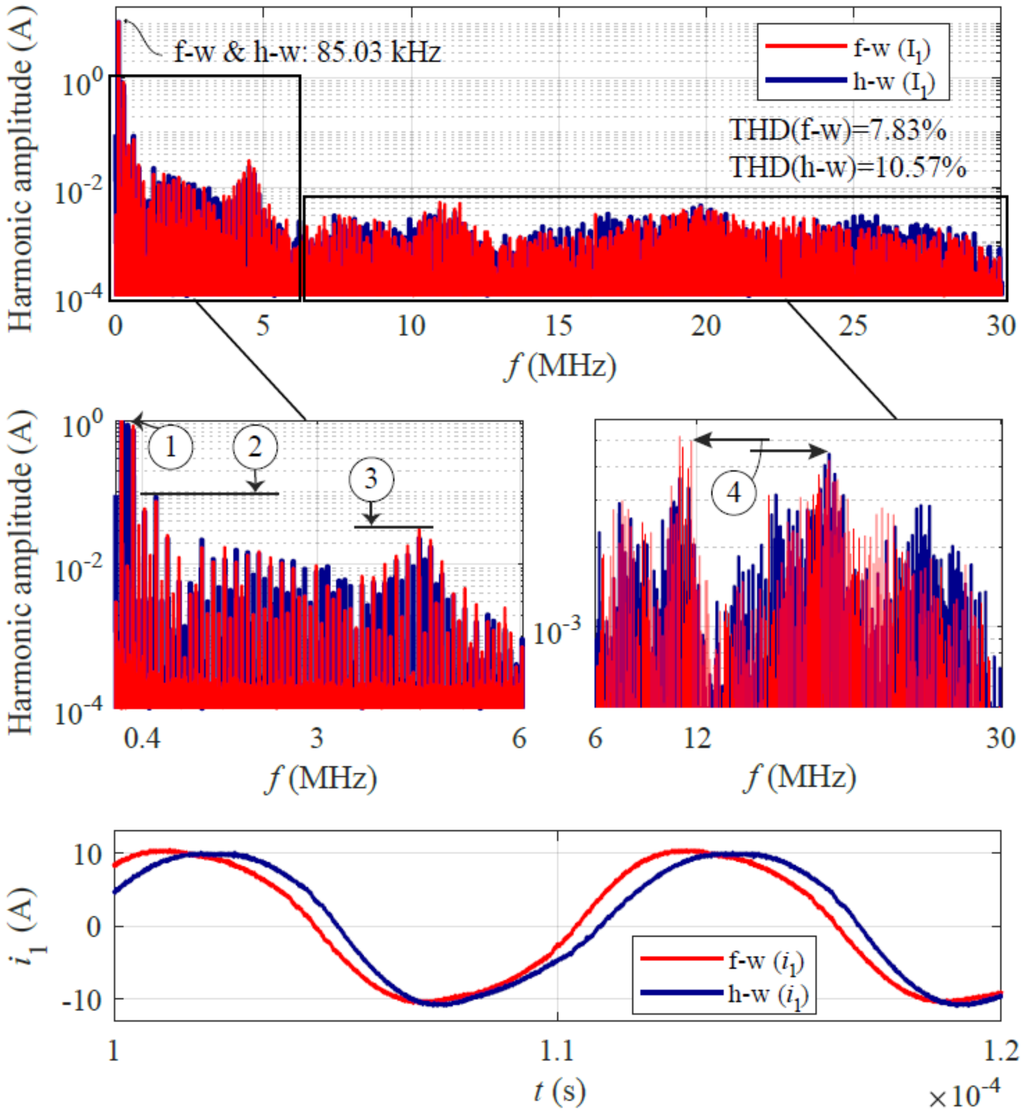

FFT of I_1: constant C and SCC with h-w modulation

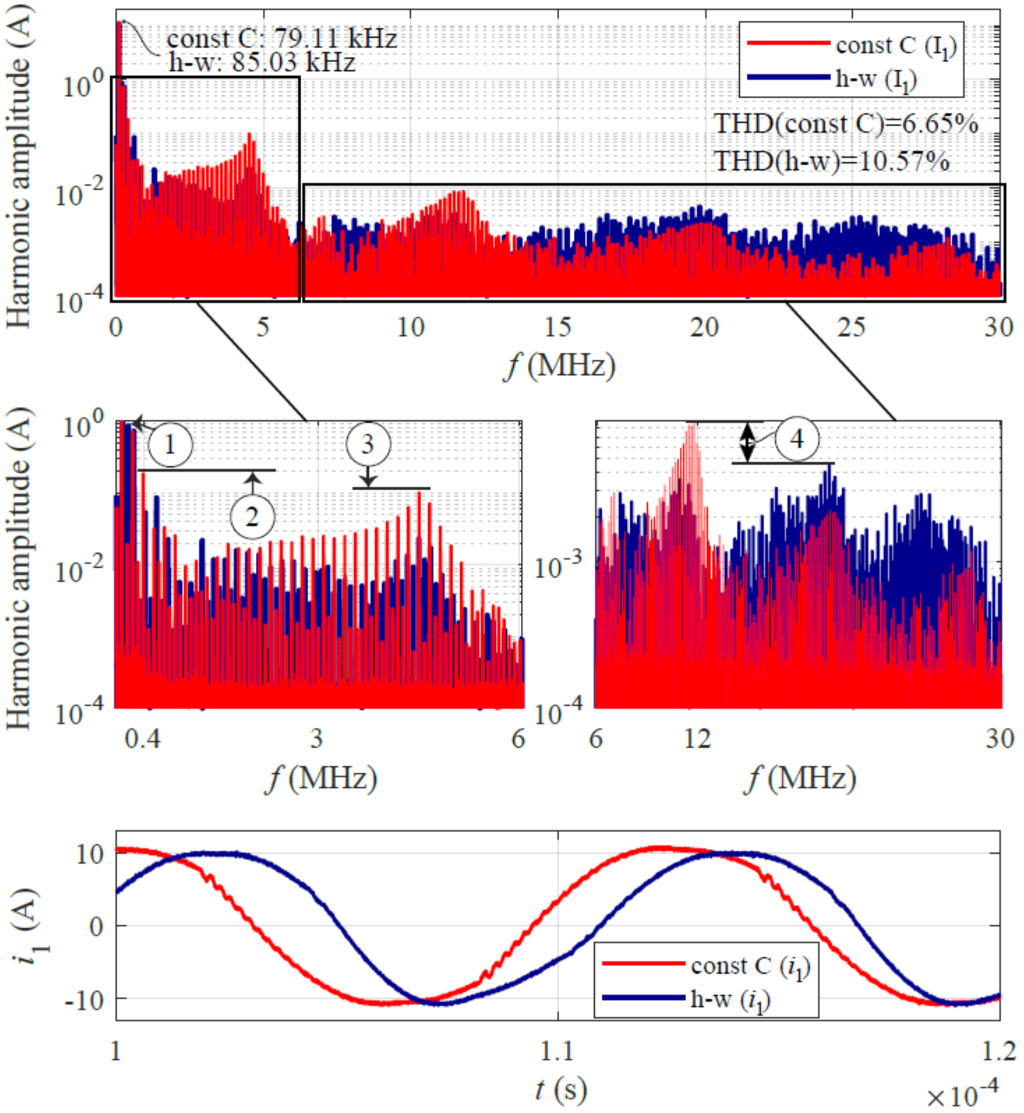

TU Delft

FEM simulation of the radiated magnetic field

Harmonic amplitude, phase and frequency of the measured I_1, I_2

↓

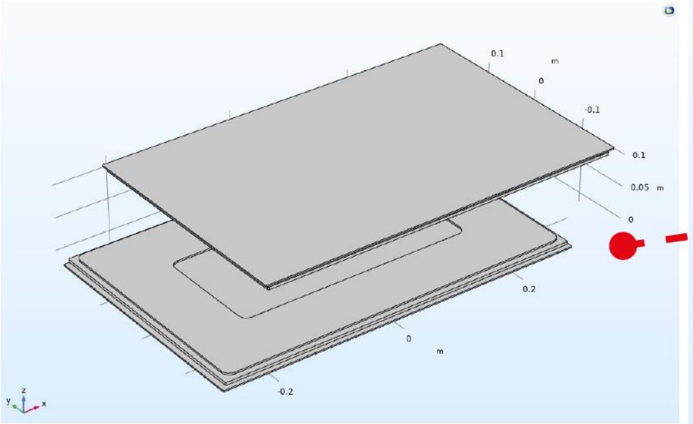

FEM model: infinite element domain

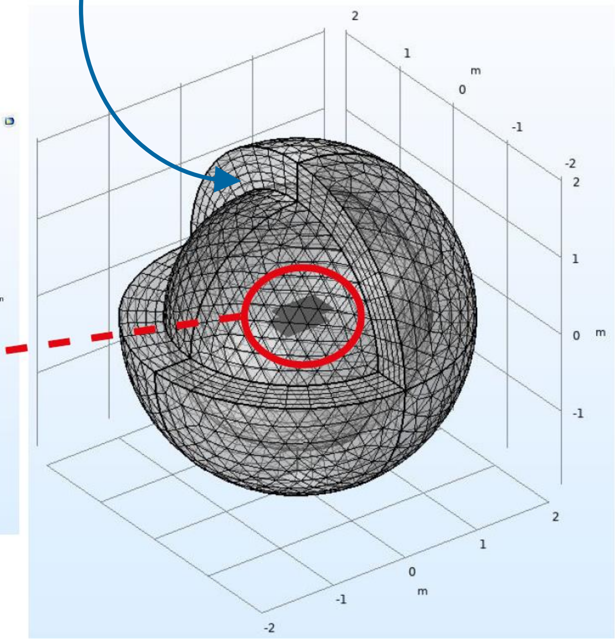

Evaluation of the radiated magnetic field

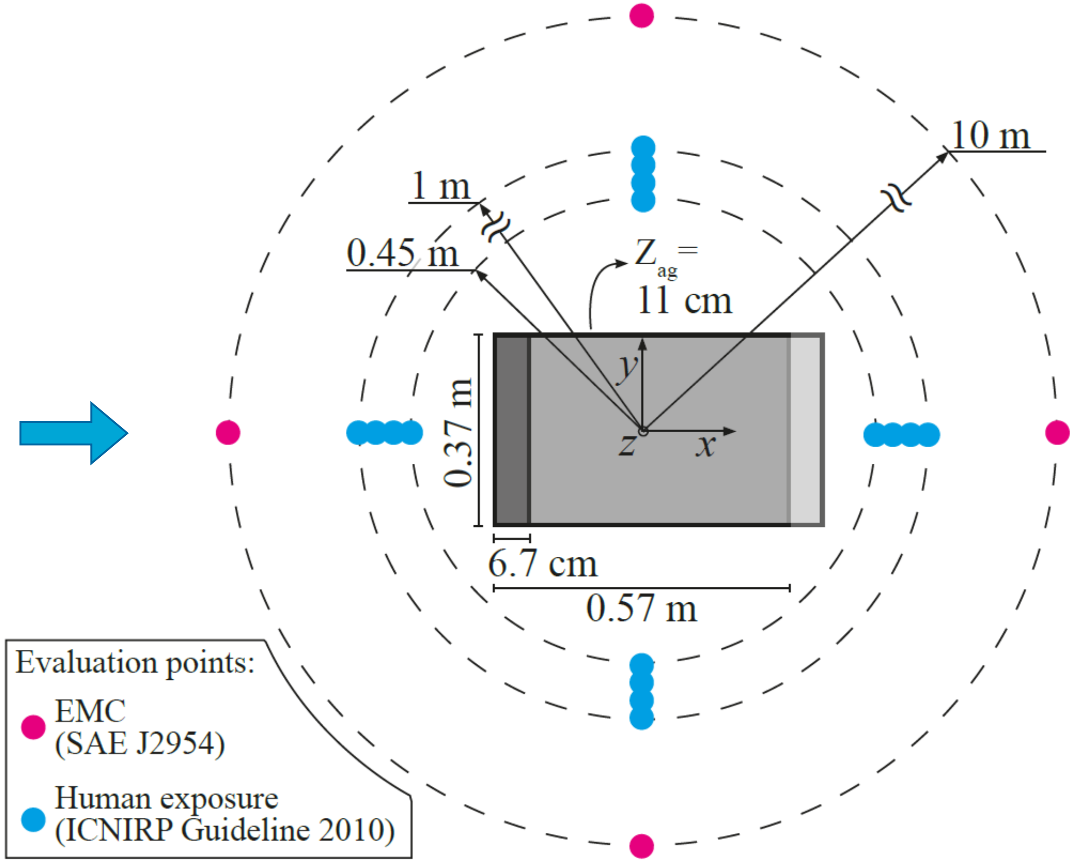

TU Delft

FEM simulation of the radiated magnetic

$$\overbrace{H_{peak}}^{(dB_{\mu A/m})} = 20 \cdot \log_{10}\left[\frac{\overbrace{B_{peak}}^{(T)}}{\mu_0} \cdot 10^6\right]$$

EMC, 10 meter distance

43 times larger B_{max} is still acceptable at the fundamental frequency

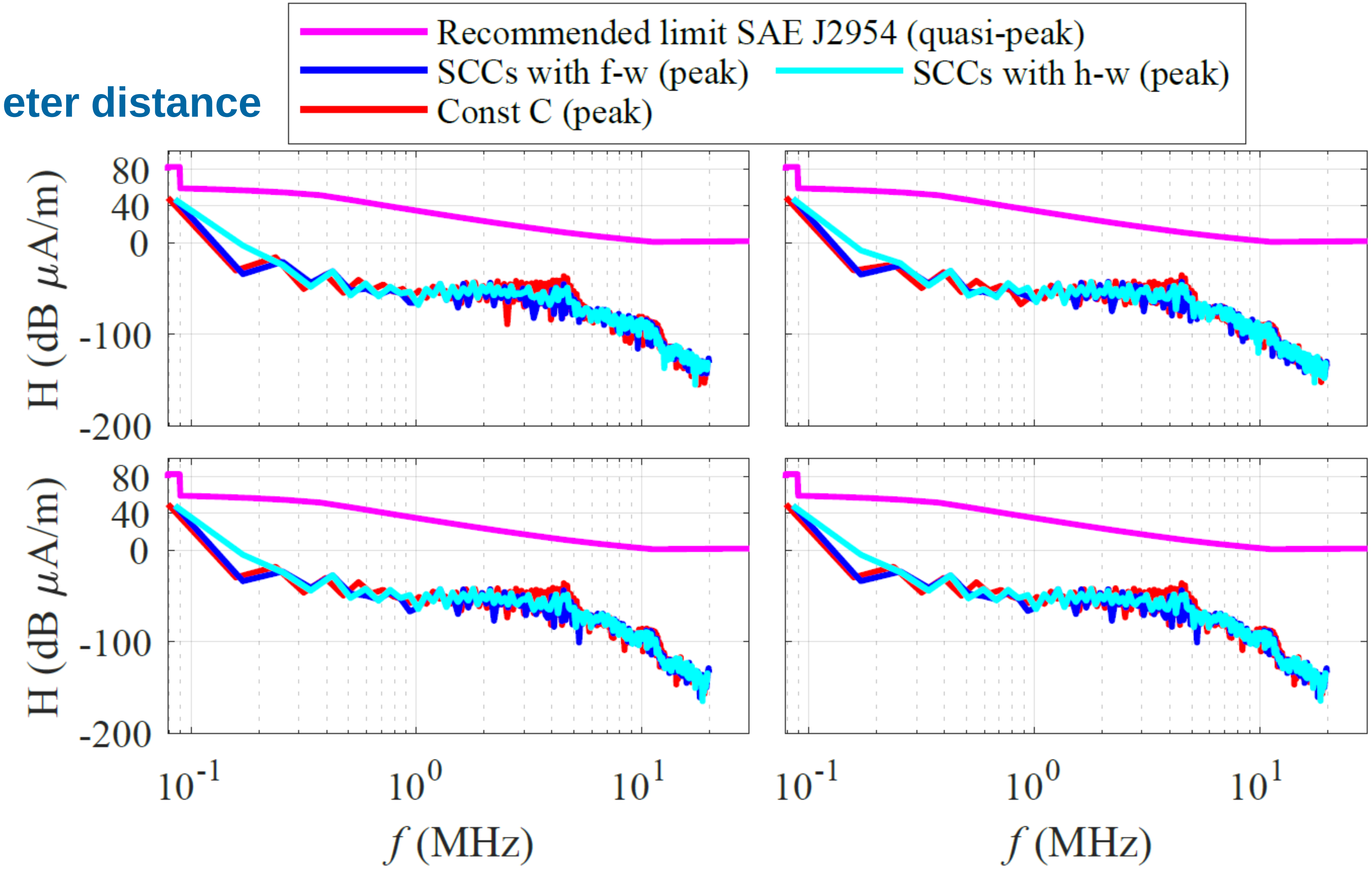

TU Delft

FEM simulation of the radiated magnetic field

Future work: experiments

Human exposure

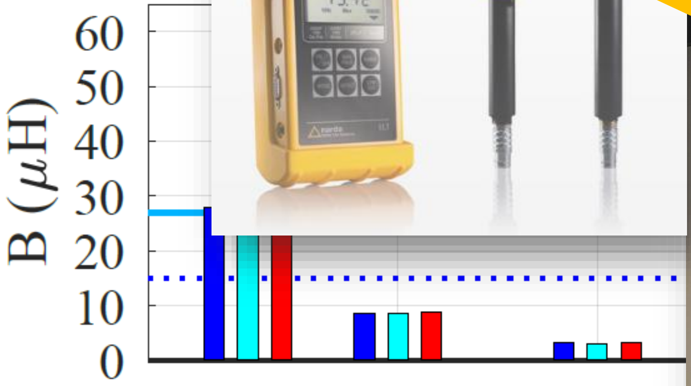

ELT-400

Exposure Level Tester
ICNIRP 1998, 1Hz-400kHz

A minimum distance of 25 cm from the outer side of the coils guarantees $B_{rms} \leq 15\ \mu\text{T}$

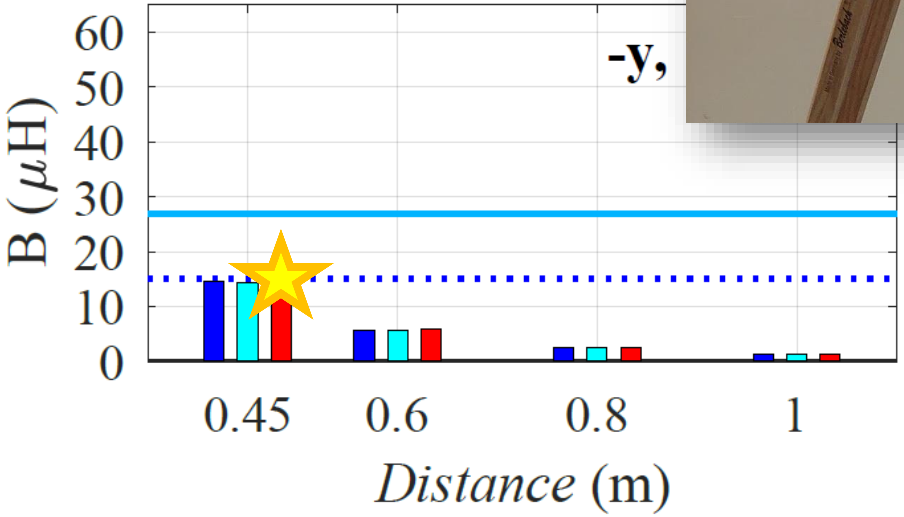

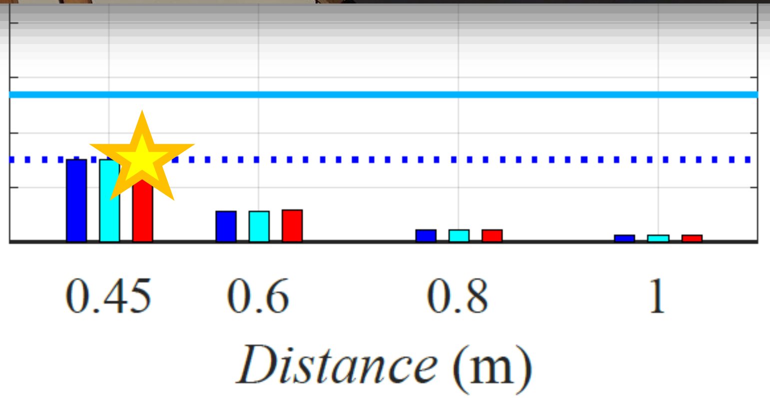

Preliminarily results

TU Delft

Conclusion and Outlook

Conclusion I

- An old (renewed) topic but thriving research
- Analysis and design: a systematic approach needed
- Possible to achieve efficiency comparable to wired charging

Wired charging:

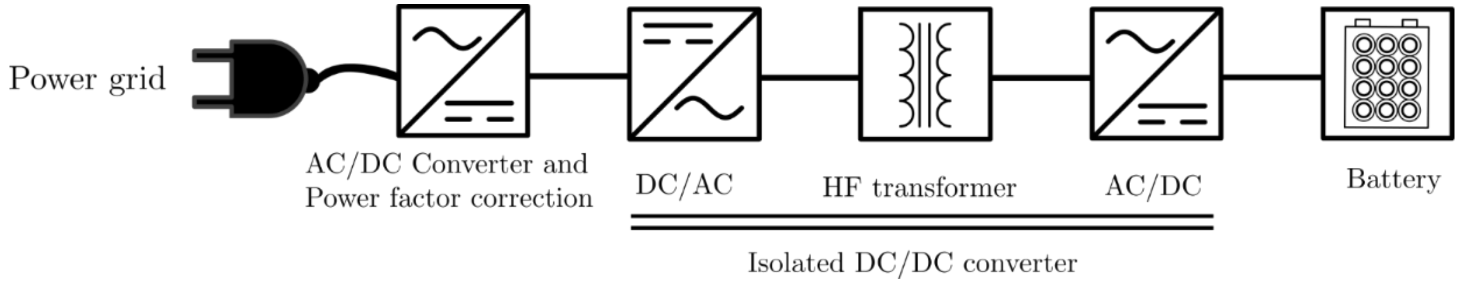

From plug to battery:

Assume: 99% efficiency each stage
Total efficiency: 99%^4 = 96%
Reality: <95% end to end

Source: H. Tao, et al. (2019), "Extreme Fast Charging of Electric Vehicles: A Technology Overview," IEEE TTE, vol. 5, no. 4.

Wireless charging:

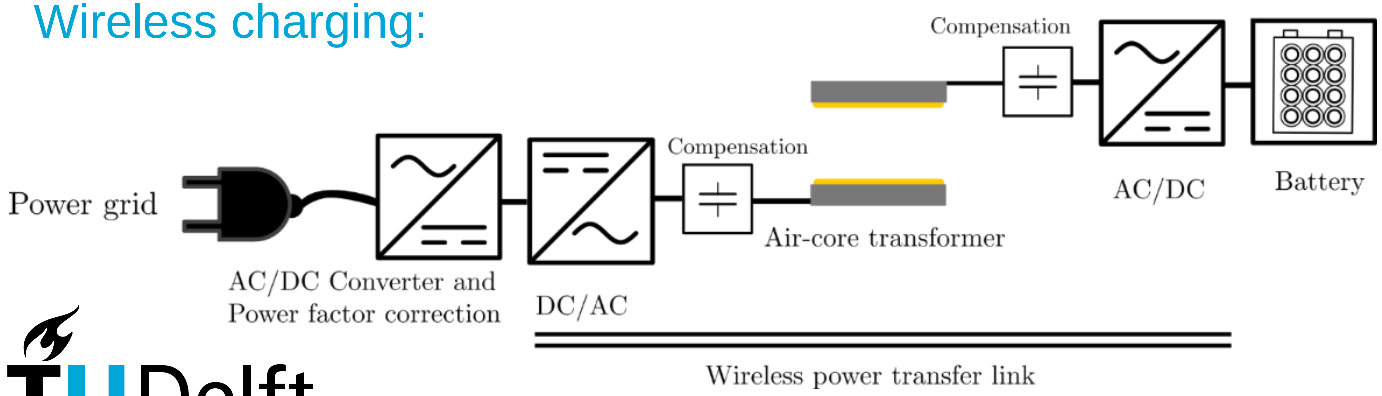

From grid to battery:

Added: two passive compensation stages (~99.7% efficient)
Replaced: HF transformer -> air-core transformer (>98% efficient)
Total efficiency: 99%^3*98%*99.7% = 95%
Reality: <95% end to end

Conclusion II

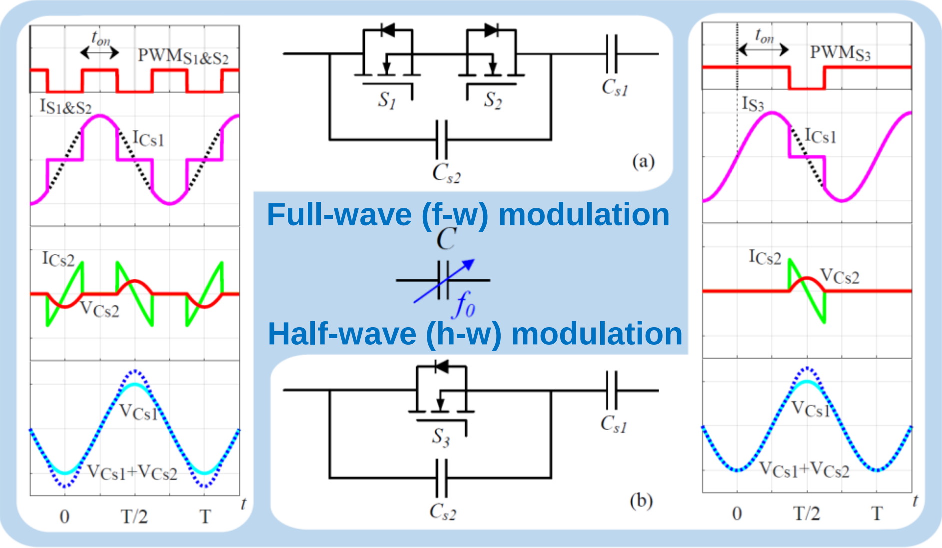

Analysis of the current distortion when SCCs are used as series compensation. 3.7kW EV wireless charging system, using:

1. SCCs with half-wave modulation,
2. SCCs with full-wave modulation,
3. Conventional fixed capacitance.

Based on:

- SCCs with half-wave modulation has the highest THD due to its asymmetrical nature. However, in correspondence with the critical frequencies of the limits set by SAE J2954, the amplitude of the single harmonic components are comparable or lower than in the other implementations. } **Measurements**
- Radiated field at 10 meters is well below the SAE J2954 recommended limits → EMC ok!
- A minimum distance of 25 cm from the outer sides of the coupled coils ensures a safe magnetic field level for both the general public and implanted medical devices according to the human exposure limits set by ICNIRP. } **FEM analysis**

TU Delft

→ Proved feasibility of using SCCs in EV wireless charging!

Outlook

Interoperability:

- Among various coils: power level/topology
- Among battery voltage levels: 400 V, 800 V …

Efficient power regulation:

- High efficient, wide voltage range DC-DC converter (front or back-end)
- Communication
- Dynamic control

Outlook

New application scenarios

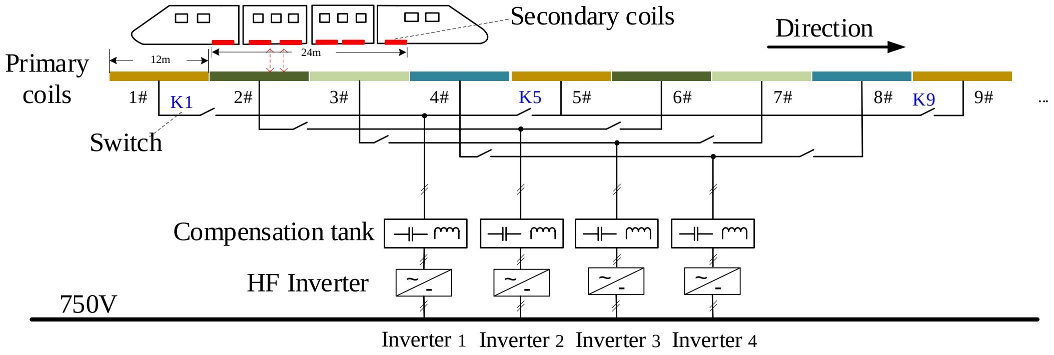

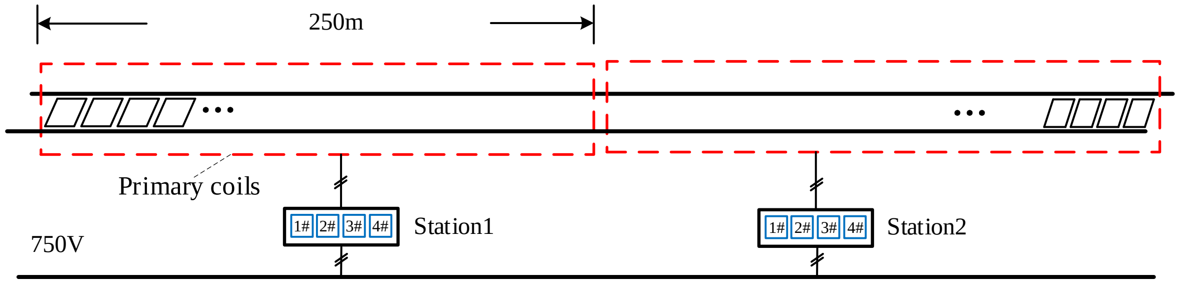

Pantograph and catenary free wireless tram, 600 kW, demonstrated in Beijing, China

Wang Z., Wang Y., et al. (2020), "A 600 kW wireless power system for the modern tram," WOW.

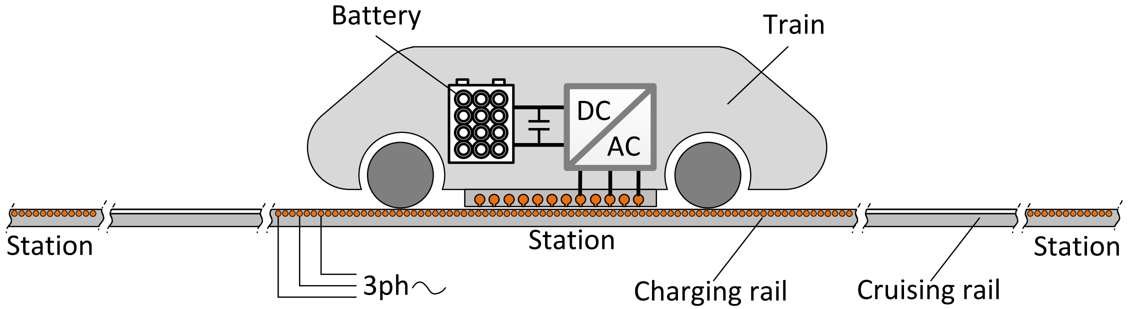

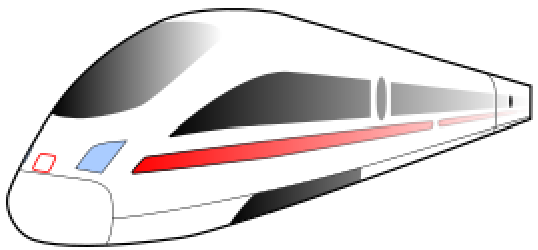

Wireless solution for ultra-high speed vacuum tube train (hyperloop), MSc study at DCE&S

Veltman A., et al. (2019), "Tunnel-Vision on Economic Linear Propulsion?," in 12th LDIA.
Becetti B. (2021), Design and optimisation of linear doubly fed induction machine for wireless charging operation of novel vactrain system, MSc thesis, TU Delft.

Thank you!

Questions?

TUDelft

Pavol Bauer
Jianning Dong
Francesca Grazian

Back-up

Inverter loss

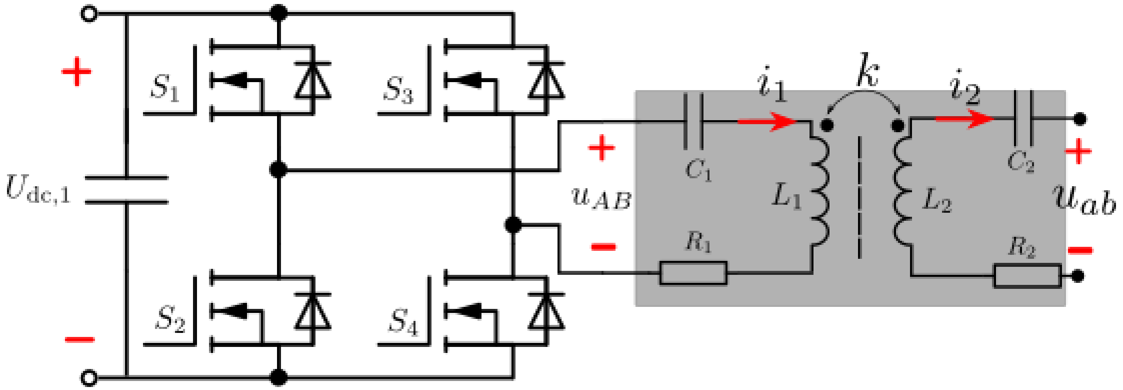

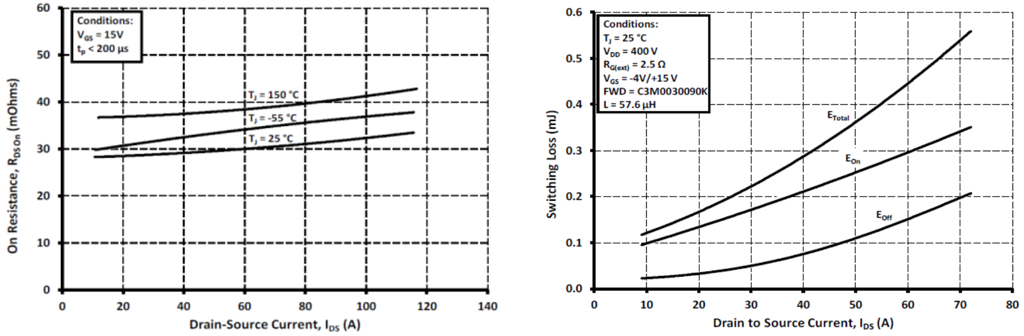

Typical conduction and switching loss curves of SiC MOSFET

P_{inv}: Fundamental frequency approximation

Conduction loss $P_{con} = 2R_{ds\_on}(T_j)I_1^2$ ⚠ temperature influence and parallel paths

Switching loss

- General H-bridge

$$P_{sw} = 2\sqrt{2}U_{dc,1}I_1\left(\frac{E_{off}+E_{on}}{V_R I_R}+\frac{Q_{RR}}{I_{RD}}\right)f_{sw}\left[\left|\cos\left(\frac{D_1\pi}{2}+\varphi_1\right)\right|\right]+\left[\left|\cos\left(\frac{D_1\pi}{2}-\varphi_1\right)\right|\right]$$

- No phase shift

Slightly inductive operation to achieve ZVS, $E_{on} = 0$

- With phase shift control

ZVS only when: $\varphi_1 > \frac{1-D_1}{2}\pi,$ soft-switching with light load requires lower power factor

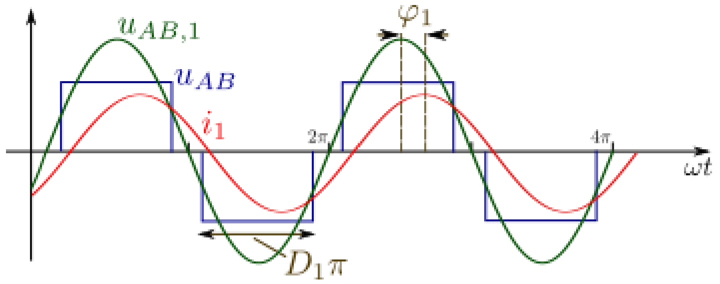

TU Delft

Li Y. et al. (2022), "A Hybrid Modulation Control for Wireless Power Transfer Systems to Improve Efficiency Under Light-Load Conditions," *IEEE Trans. Ind. Electr.*, vol. 69, no. 7, pp. 6870-6880.

Rectifier loss

Active rectifier

Same as the inverter

ZVS when:

$$\varphi_2 > \frac{1-D_2}{2}\pi$$

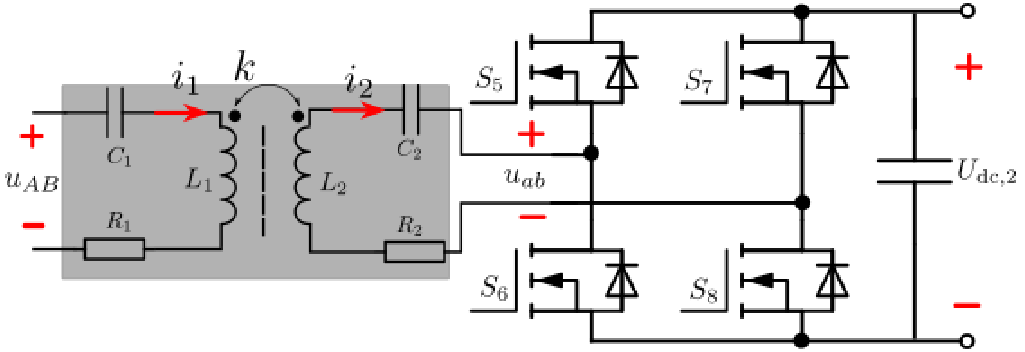

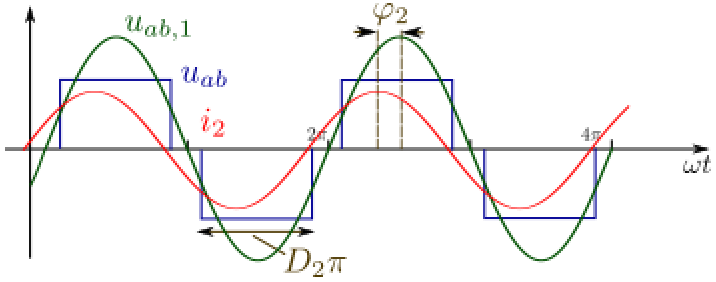

Passive rectifier

$$P_{cond,D} = 2\left(\frac{2\sqrt{2}}{\pi}V_f + r_D I_2\right)I_2$$

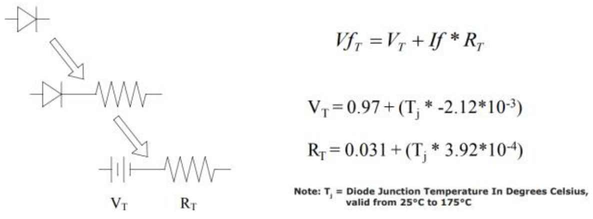

Typical diode loss model of SiC diode in datasheet

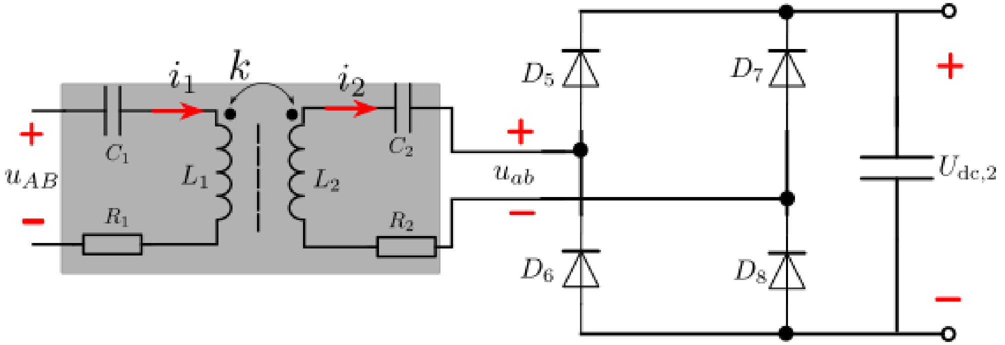

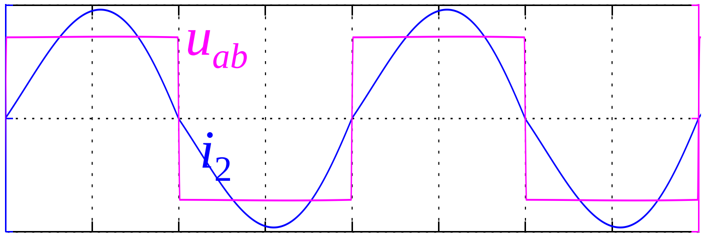

TU Delft

Compensation loss

Compensation capacitor

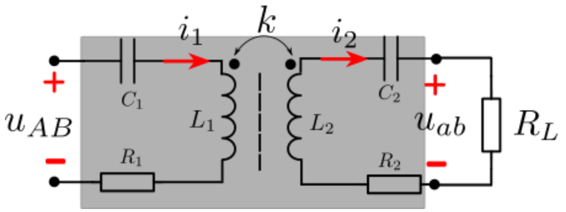

$$P_{ci} = \frac{I_i^2}{\omega C_i} \tan\delta, \quad i = 1, 2$$

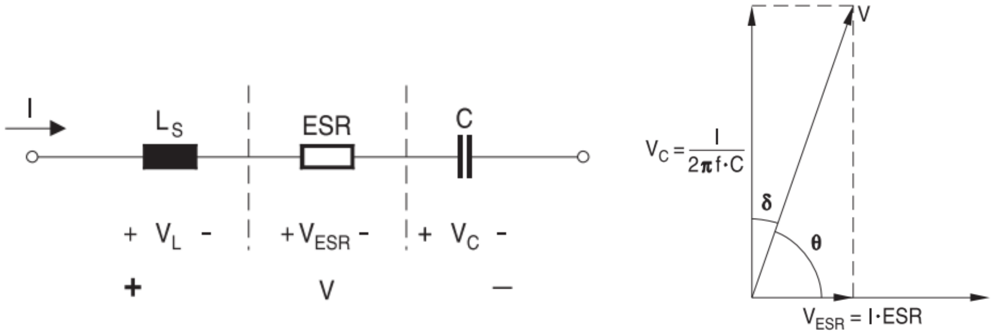

Film capacitor simplified AC equivalent circuit,
source: TDK

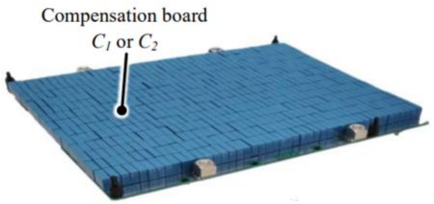

CELEM
Power Capacitors

Integrated solution to minimize parasitics

Compensation inductors

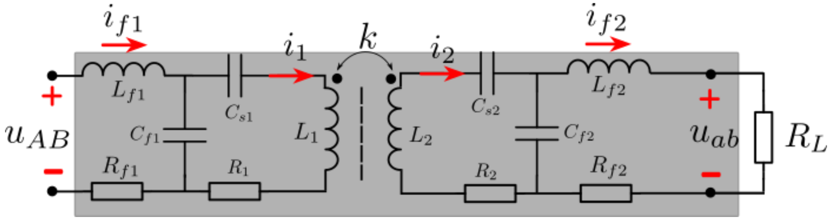

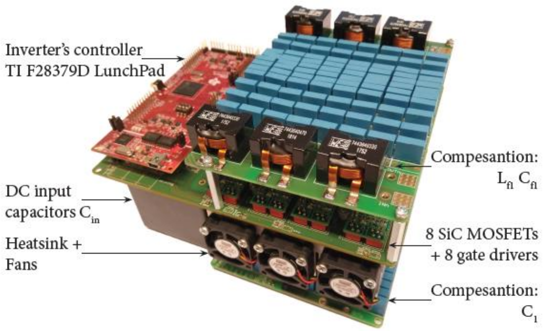

$$P_{Lfi} = I_{Lfi}^2 R_{ac,L_{fi}}, \quad i = 1, 2$$

Contributors to R_{ac}

P_{coil} : coil copper loss, DC+skin effect+approximity loss
P_{fe} : core loss, hysteresis
P_{sh} : shielding loss, eddy current loss

TU Delft

Francesca G. et al. (2020), "Compensation Network for a 7.7 kW Wireless Charging System that Uses Standardized Coils," ISCAS, 9181016].

Air-core transformer: copper loss

Electromagnetics modelling: Litz wire

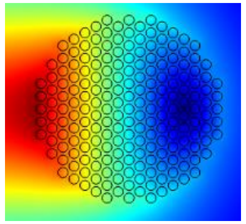

Individual strand?

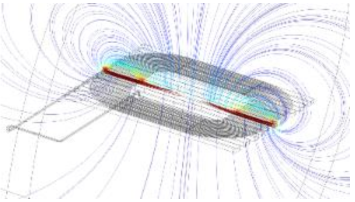

Homogenized wire
(equivalent complex permeability)

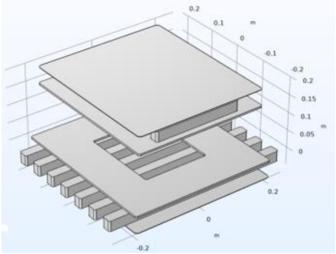

Homogeneous multi-turn coil

Guillod T., et al. (2017), Litz Wire Losses: Effects of Twisting Imperfections, COMPEL.
Xi N., et al. (2009), An Equivalent Complex Permeability Model for Litz-Wire Windings, IEEE Trans. Ind. Appl., vol. 45, no. 2.

Homogeneous coil + analytical loss calculation

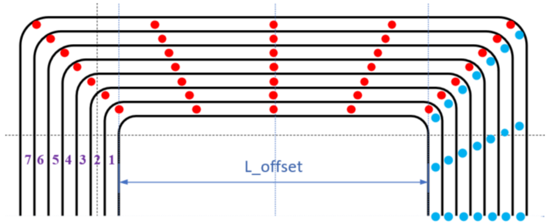

H field extraction points in 3D FEA model

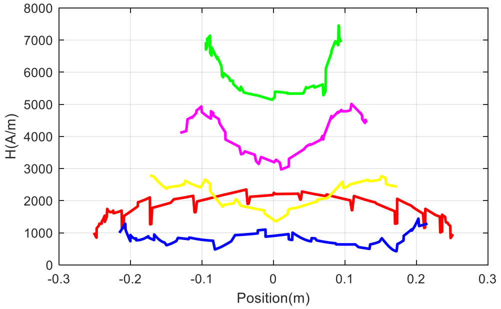

Extracted H field from FEA model

$$
\begin{cases}
P_{dc,i} + P_{skin,i} = n_{str} r_{dc} F_R\left(f_s\right)\left(\dfrac{\hat{I}_i}{n_{str}}\right)^2 L_{coil} & \text{DC+skin effect} \\
P_{pin,i} = n_{str} r_{dc} G_R\left(f_s\right)\dfrac{\hat{I}_i^2}{2\pi^2 d_a^2} L_{coil} & \text{Internal proximity effect} \\
P_{pex,i} = \displaystyle\sum_{k=1}^{N_i} n_{str} r_{dc} G_R\left(f_s\right)\oint_{l_k} \hat{H}_{ext}^2\left(l\right) dl & \text{External proximity effect}
\end{cases}
$$

Shi W., et al. (2021), “Design of a Highly Efficient 20 kW Inductive Power Transfer System with Improved Misalignment Performance”, IEEE TTE, vol. 8, no. 2.
Muhlethaler J. (2012), “Modeling and multi-objective ptimization of inductive power components,” Ph.D. dissertation, ETH Zurich.

Air-core transformer: core and shielding loss

Core loss

- Steinmetz equation
- Volumetric integral in FEA

$$P_{fe,i} = \int_{V_{fe,i}} k f_s^{\alpha} \hat{B}^{\beta} dV$$

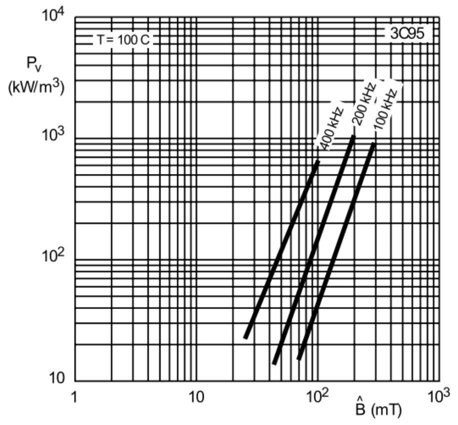

source: Ferroxcube

k = 92.66, α =1.045, β =2.44

Shielding loss

- Eddy current
- Volumetric integral in FEA

$$P_{sh,i} = \int_{V_{sh,i}} \frac{\Re\left\{\mathbf{J} \cdot \mathbf{E}^*\right\}}{2} dV$$

J: the induced current density amplitude

E: the electric field at the surface boundary

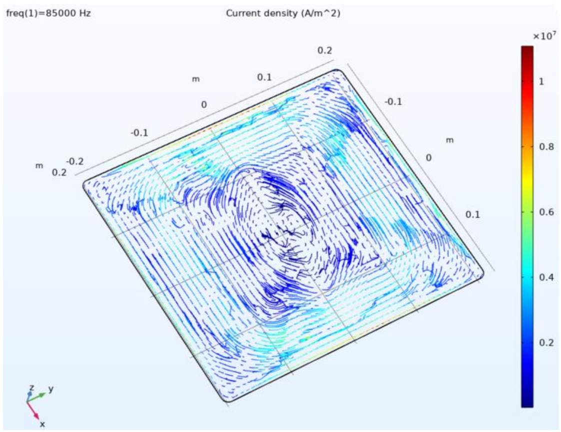

TU Delft

High efficiency 20 kW IPT system

Design requirements

Items	Symbol	Unit	Value
Output power	P_{out}	kW	20
Air gap distance	δ	mm	150
Operation frequency	f_{s}	kHz	85
DC voltage limit	$U_{\text{dc,max}}$	V	850
Lateral misalignment	Δx	mm	150

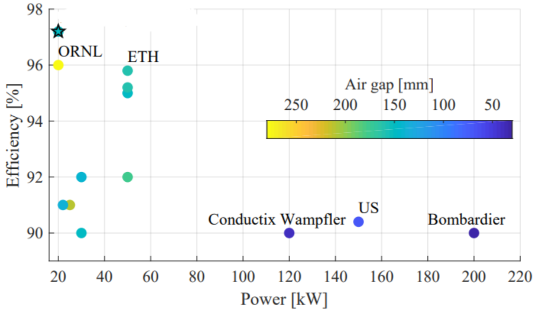

Core arrangement

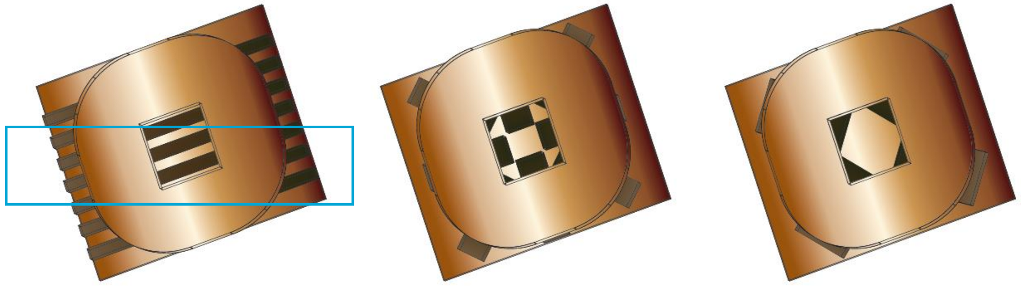

(a) Lateral placement. (b) Radial placement. (c) Cross placement.

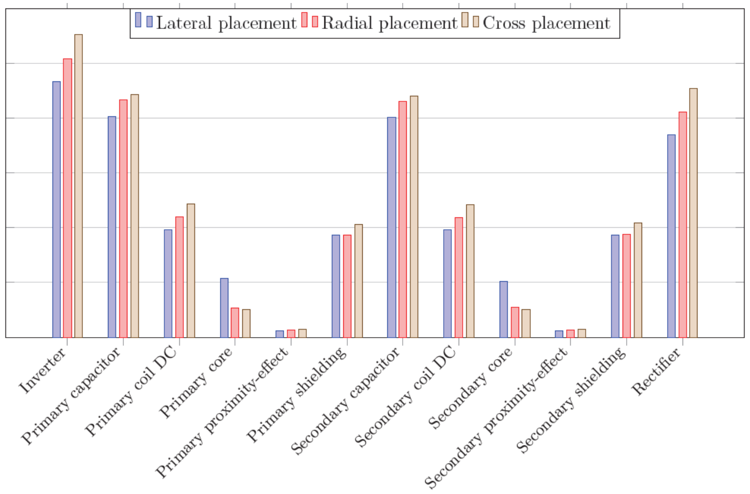

Loss comparison among various core arrangements, coils and shielding, core material and volume are kept the same

High efficiency 20 kW IPT system

Compensation selection

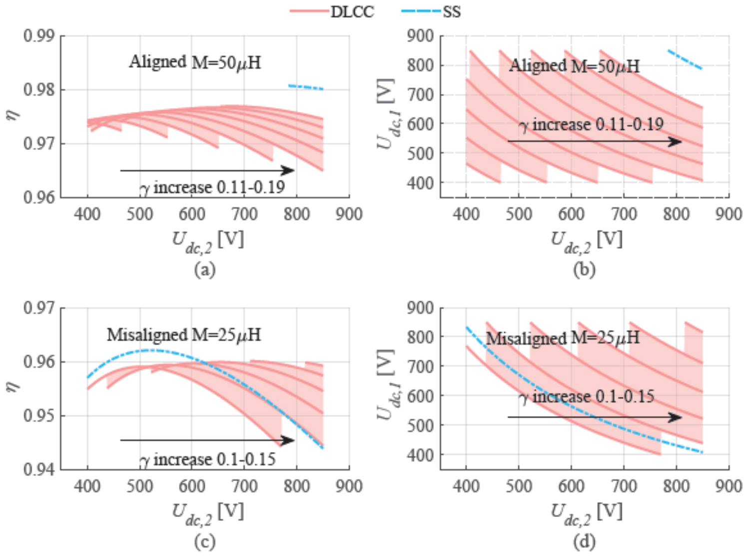

LCC-LCC vs. SS: efficiency and required primary DC voltage at 20 kW, assuming all inductors (L_i and L_{fi} have a quality factor of Q = 500)

$$\gamma = \frac{L_{f1}}{L_1} = \frac{L_{f2}}{L_2}$$

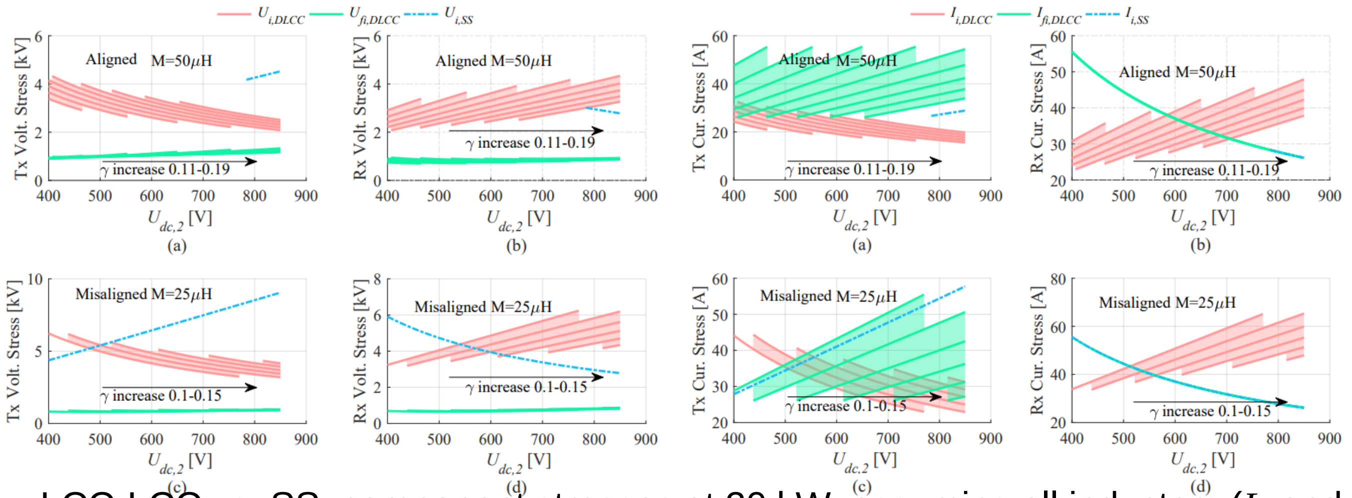

LCC-LCC vs. SS: component stresses at 20 kW, assuming all inductors (L_i and L_{fi} have a quality factor of $Q = 500$)

Conclusion

- LCC-LCC efficiency dependent on γ
- Maximum efficiency S-S is higher
- S-S: high M leads to limited voltage range to achieve rated power
- LCC-LCC: large γ gives high efficiency, but limits voltage range

- S-S is selected for its higher efficiency with similar voltage stress

Shi W., et al. (2021), “Design of a Highly Efficient 20 kW Inductive Power Transfer System with Improved Misalignment Performance”, IEEE TTE, vol. 8, no. 2.

High efficiency 20 kW IPT system

Power converters

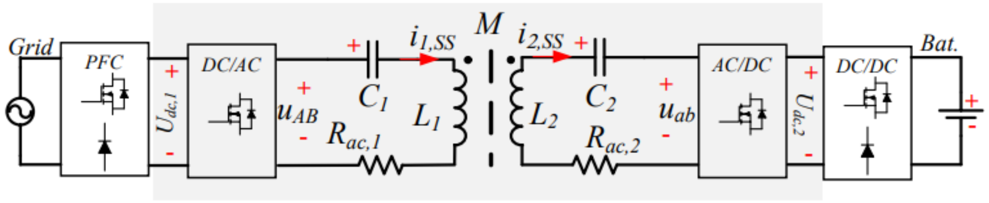

- Active H-bridges on both sides
- Power regulation via PFC output voltage
- Back-end DC-DC for impedance matching

Minimizing switching losses in IPT inverter and rectifier

Search space

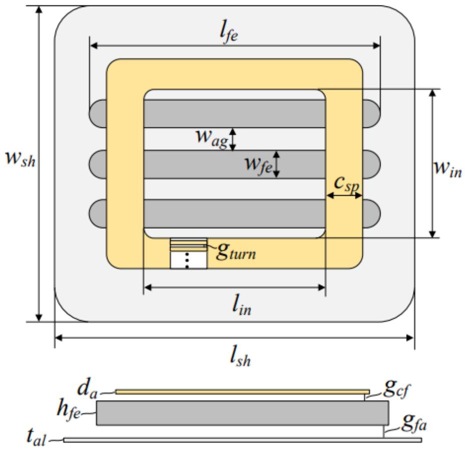

Variables	Symbol	Unit	Range
Number of turns	N	-	10-35
Number of ferrites	n_{fe}	-	5-9
Inner length	l_{in}	mm	25-300
Inner width	w_{in}	mm	25-300
Ferrite thickness	h_{fe}	mm	5-35
Ferrite width	w_{fe}	mm	15-45
Relative ferrite length	$l_{\mathrm{fe,r}}$	%	50-150
Relative gap between ferrites	$w_{\mathrm{ag,r}}$	%	10-100
Gap between coil and ferrites	g_{cf}	mm	0.1-5
Gap between ferrites and shielding	g_{fa}	mm	1-20
Gap between coil turns	g_{turn}	mm	1-3

DCE&S
DC systems, Energy conversion & Storage

TU Delft

High efficiency 20 kW IPT system

Design objectives

- Maximize: Aligned efficiency η_{al}
- Maximize: Misaligned efficiency η_{mis}
- Minimize: Receiver pad area ρ_A
- Minimize: Total system weight (Tx+Rx assembly) ρ_G

Constraints

- Winding current density < 5 A/mm^2
- Ferrite flux density < 350 mT

Optimisation procedure

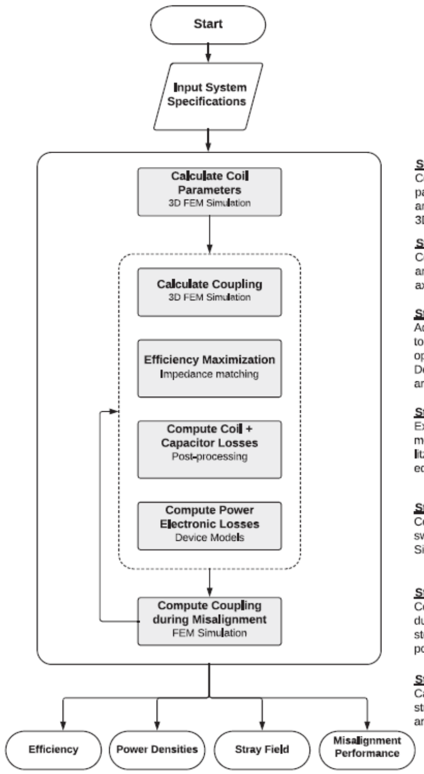

Step 1
Compute the self-inductance and parasitic resistances of the transmitter and receiver coils using axi-symmetric 3D FE models.

Step 2
Compute the mutual inductance (M) and coupling co-efficient (k) using axi-symmetric / full 3D FEM models.

Step 3
Adapt the operating dc link voltages to maximize efficiency based on optimal load matching algorithm. Derive the coil driving currents analytically.

Step 4
Extract magnetic field data from FE model to compute coupler losses: litz copper loss, core loss, aluminium eddy loss.

Step 5
Compute the losses in the hard switched inverter and the rectifier with Si-C switch and diode loss models.

Step 6
Compute the coupling co-efficient (k') during misalignment. Repeat step 2 - step 5 to determine the new operating point and associated losses.

Step 7
Calculate the transmission efficiency, stray field, coupler active mass and area, and the misalignment tolerance.

- Both aligned and misaligned conditions are evaluated

Bandyopadhyay S., et al. (2019), "Comparison of Magnetic Couplers for IPT-Based EV Charging Using Multi-Objective Optimization," *IEEE TVT*, vol. 68, no. 6, pp. 5416–5429.

High efficiency 20 kW IPT system

Tradeoffs

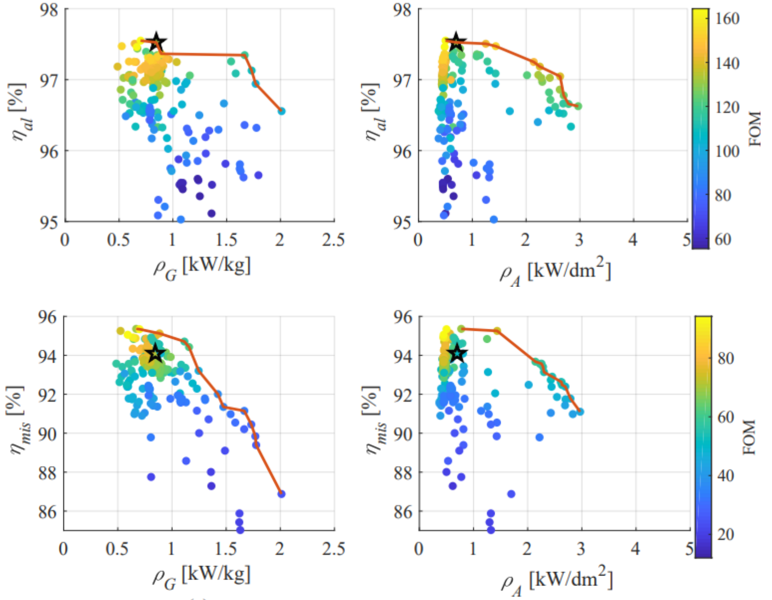

(a) (b)

- Figure-of-merit:

$$FOM = kQ, \quad Q \text{ is the coil quality factor}$$

- Overall higher FOM, higher efficiency
- Exemption because capacitor loss is larger

Final design

Variables	Symbol	Unit	Tx/Rx
Number of turns	N	-	23/31
Number of ferrites	n_{fe}	-	7/5
Inner length	l_{in}	mm	184.7/66.2
Inner width	w_{in}	mm	220.8/114.2
Ferrite thickness	h_{fe}	mm	28.8
Ferrite width	w_{fe}	mm	27.7
Ferrite length	l_{fe}	mm	515.3/243.1
Gap between ferrites	w_{ag}	mm	41.8/69.3
Gap between coil and ferrites	g_{cf}	mm	3.9/1
Gap between ferrites and shielding	g_{fa}	mm	10.6/15.0
Gap between coil turns	g_{turn}	mm	2.2

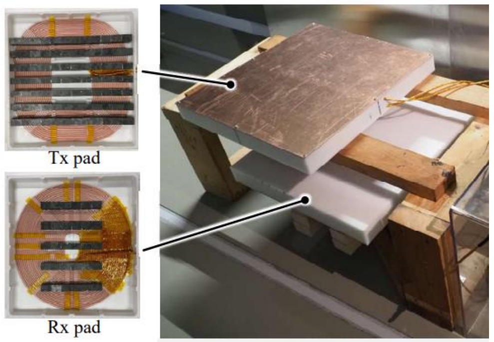

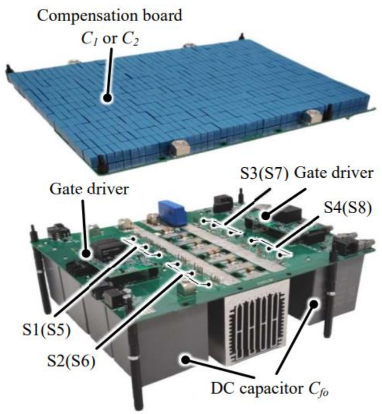

DC systems, Energy conversion & Storage

Motivation

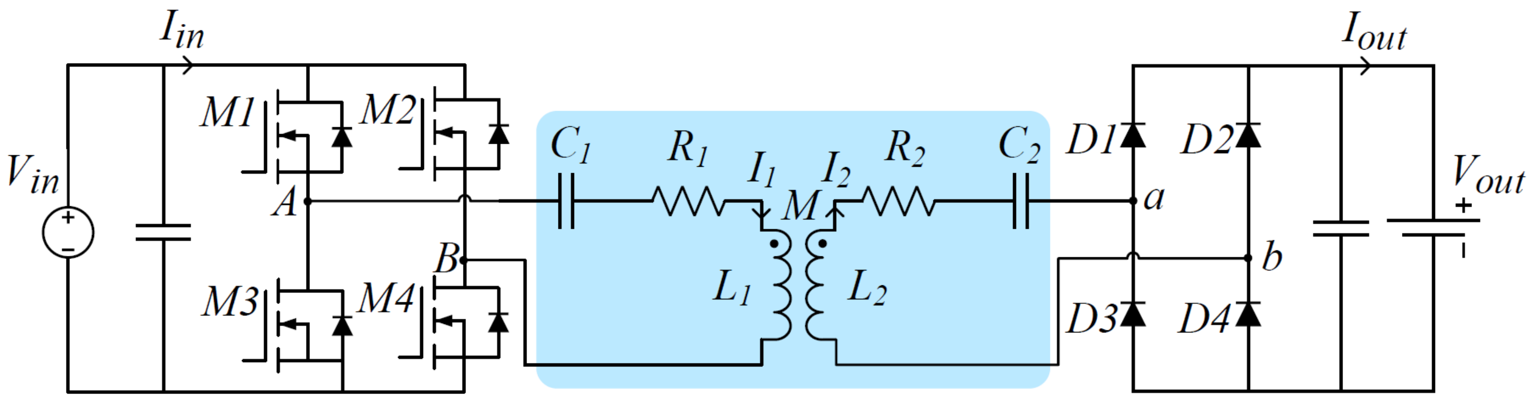

Two main challenges:

→ **High power transfer efficiency** throughout the whole EV battery charging profile

Switch-controlled capactiors (SCC) as series compensation

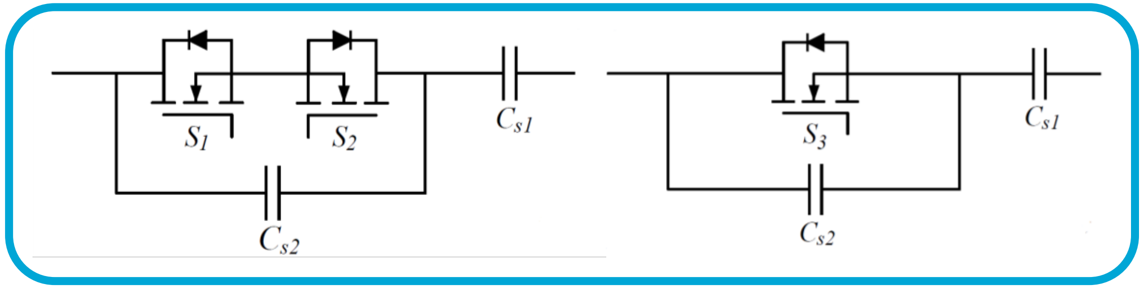

→ Currents (I_1 and I_2) distortion?

→ The **magnetic field** is not harmful to the living beings in the surroundings and is lower than the recommended EMC limits

TU Delft

Objective

To analyze the current distortion caused by the SCCs to achieve constant optimum load (COL) matching at different coils' alignments.

Optimum load matching

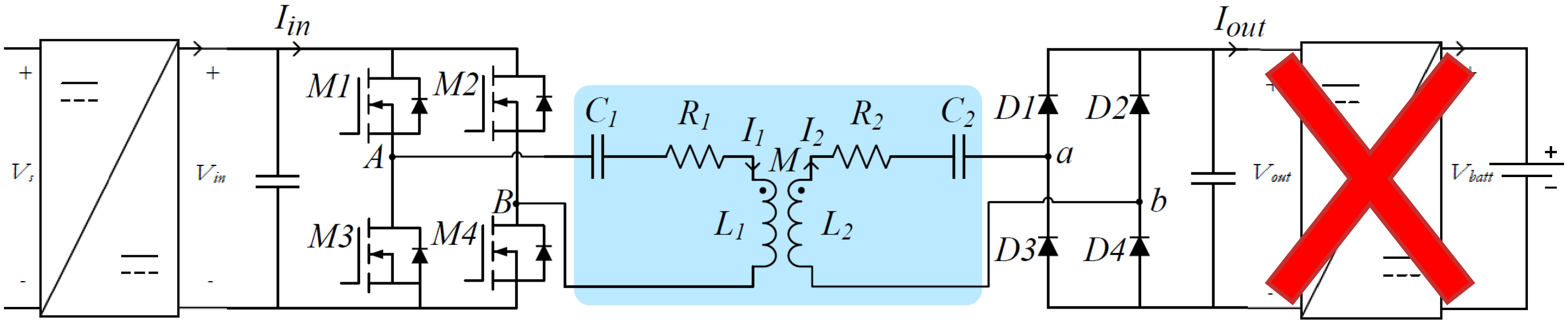

Optimum equivalent resistive load: [1]-[3]

$$R_{L,opt} = \frac{\pi^2}{8}\omega_0 M \sqrt{\frac{R_2}{R_1}}$$

Dependence on the coils' alignment

$M \downarrow \ \rightarrow \ R_{L,opt} \downarrow \ \rightarrow$ control of V_{out} :

$$R_L = \frac{V_{out}}{I_{out}} = R_{L,opt}$$

Output power:

$$P_{out} = V_{out}\ I_{out} = \frac{8}{\pi^2}\frac{V_{in}\ V_{out}}{\omega_0\ M}$$

$M \downarrow \ \rightarrow \ P_{out} \uparrow \ \rightarrow$ control of V_{in} :

$$P_{out} = P_{out}^*$$

[1] R. Bosshard, J. W. Kolar, J. Mühlethaler, I. Stevanovic, B. Wunsch, and F. Canales, "Modeling and η-α-pareto optimization of inductive power transfer coils for electric vehicles," *IEEE Journal of Emerging and Selected Topics in Power Electronics*, vol. 3, pp. 50 – 64, 2015.

[2] S. Bandyopadhyay, P. Venugopal, J. Dong, and P. Bauer, "Comparison of magnetic couplers for ipt-based ev charging using multi-objective optimization," *IEEE Transactions on Vehicular Technology*, vol. 68, no. 6, pp. 5416–5429, 2019.

[3] F. Grazian, W. Shi, T. B. Soeiro, J. Dong, and P. Bauer, "Electric vehicle charging based on inductive power transfer employing variable compensation capacitance for optimum load matching," in *IECON 2020 The 46th Annual Conference of the IEEE Industrial Electronics Society*, 2020, pp. 5262–5267.

TU Delft

Constant optimum load through variable series compensation

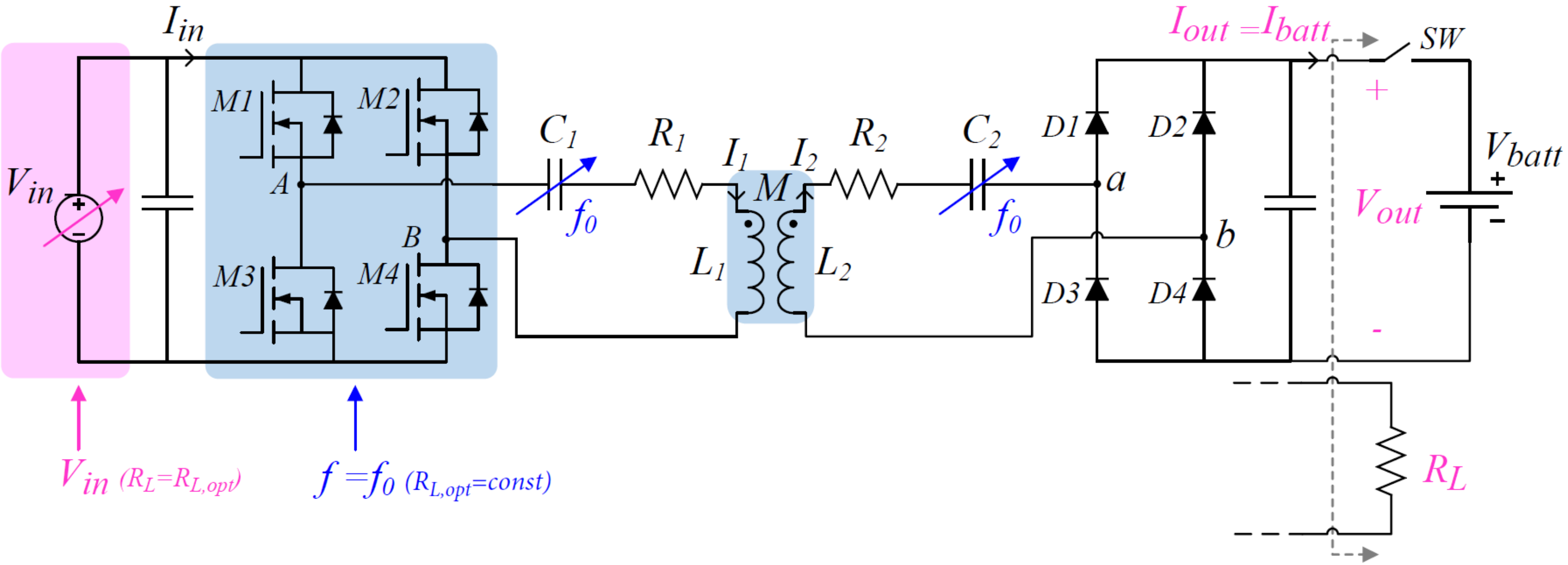

Fixed over M variations

$$R_{L,opt} = \frac{\pi^2}{8}\omega_0 M\sqrt{\frac{R_2}{R_1}}$$

$$P_{out} = V_{out}\ I_{out} = \frac{8}{\pi^2}\frac{V_{in}\ V_{out}}{\omega_0 M}$$

$M\downarrow \ \rightarrow\ \omega_0\uparrow$

Proposed method:

Control of the system's natural resonant frequency

↓

Constant optimum load (COL) over different *M*

More info, **accepted paper** in IEEE Journal of Emerging and Selected Topics in Power Electronics

"Inductive Power Transfer based on Variable Compensation Capacitance to Achieve an EV Charging Profile with Constant Optimum Load"

TU Delft

Constant optimum load through variable series compensation

Misalignment

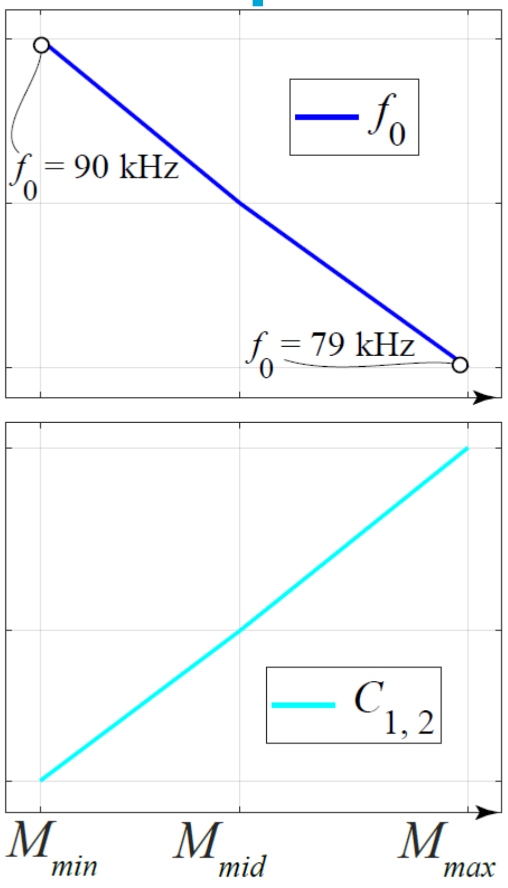

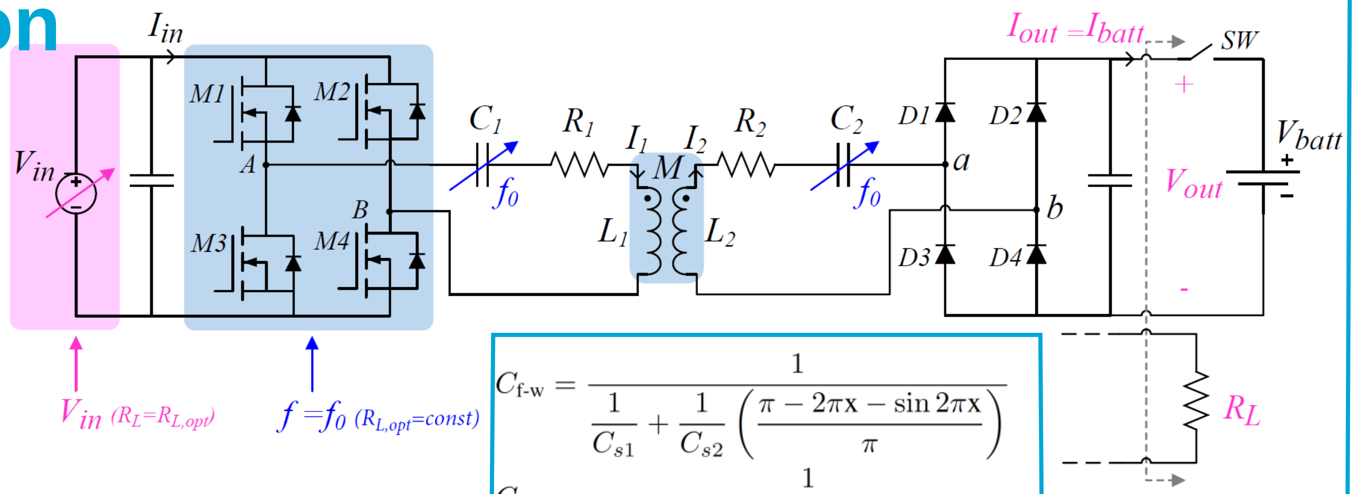

$$C_{\text{f-w}} = \frac{1}{\left(\frac{1}{C_{s1}} + \frac{1}{C_{s2}}\right)\left(\frac{\pi - 2\pi x - \sin 2\pi x}{\pi}\right)}$$

$$C_{\text{h-w}} = \frac{1}{\left(\frac{1}{C_{s1}} + \frac{1}{C_{s2}}\right)\left(\frac{2\pi - 4\pi x + \sin 4\pi x}{2\pi}\right)}$$

Switch-controlled capacitor (SCC) as compensation

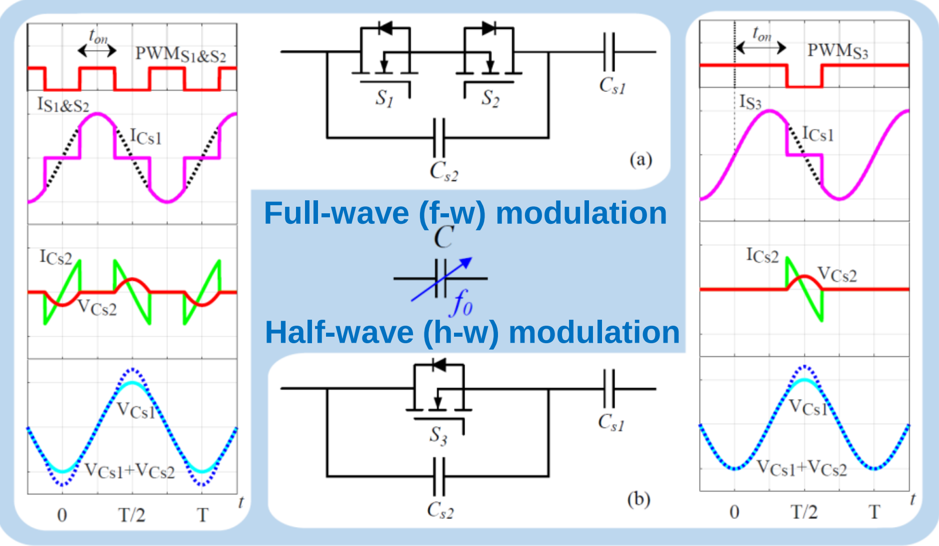

Charging profile

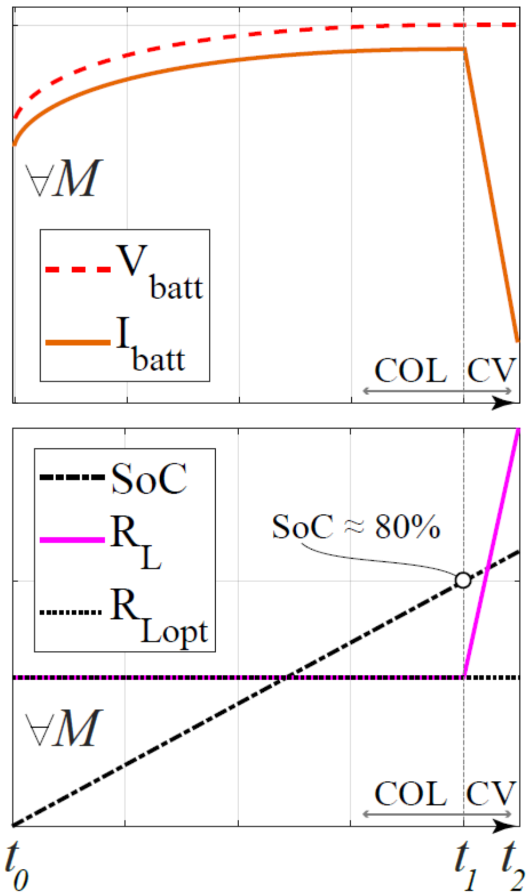

COL charging profile

(V_{in} control through the grid-connected PFC converter)